Evaluation of Lignin-containing Photopolymers for use in Additive Manufacturing

A Thesis Presented for the

Master of Science

Degree

The University of Tennessee, Knoxville

Jordan Thomas Sutton

August 2019

ACKNOWLEDGEMENTS

I would like to thank Dr. Stephen Chmely and Dr. David Harper for giving me the opportunity to pursue this work and for all the guidance and support they have provided during my time here. Special thanks to Dr. Kalavathy Rajan for helping me in too many ways to count and for being a great friend. I would like to thank Dr. David Keffer for both serving on my committee and for assisting me in finding a place here in graduate school. I would also like to thank Chris Helton, Dr. Nicole Labbé, and Dr. Chris Wetteland, as well as all my friends at the Center for Renewable Carbon and the Material Science and Engineering Department.

ABSTRACT

Generating high value products from lignin has been the goal of decades of research attempting to use the abundant byproduct of paper and biofuel production. Lignin's complex aromatic structure means that it can potentially act as a feedstock for chemicals, fuels, and polymers. Bio-based polymers are a focus of discussion given the increasing concerns over polymer waste and renewability. For these reasons, efforts have been made to develop polymer products using lignin as an additive or a functionalized part of the polymer network. Photopolymerizable materials have been largely excluded from these works due to perceived difficulties understanding lignin's photoactive structure. In this study, we show that lignin can be used in commercial photopolymer products with an emphasis on resins for stereolithography and can be modified to tune photoactive properties. The first section of this work features the generation and characterization of lignin photo-active stereolithography resins. With methacrylic modification, it was possible to print with resins loaded with up to 15% lignin by weight on a commercial desktop 3D printer. However, thermal and cure properties were degraded by the addition of lignin. In the second section, different modification techniques were studied to improve cure properties in lignin photopolymers. A combination of reduction and acylation modifications greatly increased UV transparency and reduced critical cure dosage. Mechanical stiffness and strength were also improved due to lignin increasing cross-link density. These findings provide a basis for lignin's application in photopolymers for additive manufacturing.

PREFACE

This manuscript consists of four chapters: a general introduction, two research articles, and collected conclusions. The first of the research articles is a version of a manuscript published in the American Chemical Society journal for "Applied Materials & Interfaces". The second article is an in-progress work for publication. The articles can stand alone as cohesive works, but they are incorporated here as chapters to present the main objectives of this study.

Chapter 1 provides an overview of lignin sources, structural characteristics, and modification techniques, as well as background on additive manufacturing, photopolymer composition, characterization, and applications of lignin acrylate photopolymers, to assist the reader with understanding of the importance of lignin as a biopolymer feedstock source.

Chapter 2 explores modification, characterization, and processing techniques used for developing lignin-containing photoactive resins for stereolithography printing. Methodology and characterization of the modifications to lignin and its incorporation in photopolymer resin are given here to assist in relate the chemical and structural changes to the resultant material behavior. Material preparation and characterization were performed at the Center for Renewable Carbon at the University of Tennessee Institute of Agriculture (UTIA).

Chapter 3 presents a study of modification techniques to improve upon cure properties in lignin acrylate photopolymers using UV-vis, FTIR, and NMR spectroscopy to observe chemical changes that affect UV absorptivity. This work builds upon what was done in Chapter 2 and attempts to solve problems discovered in the previous study.

Chapter 4 gathers conclusions on the applications of lignin toward photopolymers from the results of the various experiments conducted and the significance of this work. Future work to continue the development of lignin in photopolymers is also discussed.

TABLE OF CONTENTS

LIST OF TABLES

LIST OF FIGURES

ABBREVIATIONS AND SYMBOLS

AM = Additive Manufacturing
ASTM = American Society for Testing and Materials
ATR = Attenuated Total Reflectance
C = Carbon
DED = Directed Energy Deposition
DLP = Digital Light Processing
D_p = Penetration Depth
E = Young's Modulus
E_c = Critical Cure Dosage
FDM = Fused Deposition Modeling
FTIR = Fourier-transform infrared
GCP = Gel Permeation Chromatography
LR = Lignin Resin
NMR = Nuclear Magnetic Resonance
PCA = Principal Component Analysis
Pl = Laser Power
SEM = Scanning Electron Microscope
SLA = Stereolithography Apparatus
SLS = Selective Laser Sintering
TGA = Thermogravimetric Analysis
UTS = Ultimate Tensile Strength
UV = Ultraviolet

CHAPTER 1

INTRODUCTION

LIGNIN

Natural Lignin and Its Structure

The three main components of plant cell walls are cellulose, hemicellulose, and lignin. These compounds and their structure within the plant determine the physicochemical properties necessary for the organism's survival. The functions they serve include contributing to the physical integrity and shape of the plant, resisting pathogens, regulating cell growth, and controlling the passage of water and nutrients. The cellulose forms into bundles shaping the framework of the cell wall, while hemicellulose and lignin fill in fibers connecting the cellulose bundles. This accounts for the majority of the total plant biomass, which is the largest part of the biomass on Earth [1].

Lignin is the second-most abundant natural polymer, behind cellulose, with a relatively high carbon content, accounting for approximately 30% of all organic carbon in the biosphere [2]. It is an inhomogeneous group of complex substances composed of phenylpropane groups. Lignin is generally formed by the polymerization of three primary monomeric alcohols: *p*-coumaryl, coniferyl, and sinapyl. The various combinations of these monomers lead to the categorization of lignin subunits into *p*-hydroxyphenyl (H), guaiacyl (G), and syringyl (S). Typically, lignin from gymnosperms consist mainly of guaiacyl lignin (G), dicotyledonous angiosperms have a mixture of guaiacyl and syringyl lignin (GS), and monocotyledonous angiosperms have a mixture of all three types (GSH) [2]. Likewise, the amount of lignin can vary based on the source; softwoods contain up to 28% lignin, hardwoods up to 20%, and grasses up to 19%.

Lignin is a unique biopolymer because it lacks a defined principal structure and is highly heterogeneous. Different plant sources show various linkages and compositions of functional groups. Due to the destructive processes in most lignin isolation techniques, it is difficult to determine a primary structure even for lignin from the same plant. Much work has been done to study and produce models for the structure of lignin [3, 4]. Generalized, lignin is a complex amorphous polyphenolic polymer with a crosslinked three-dimensional network. It is composed of phenylpropane groups, primarily coumaryl alcohol, coniferyl alcohol, and sinapyl alcohol, linked by C-O and C-C bonds. Beyond this, it is necessary to study and characterize the specific lignin sources of interest and adapt processing to accommodate differences.

Extraction Techniques

Currently, most commercially available lignin is produced as a by-product of pulp mills. These mills produce paper and other cellulose-based materials using pulping techniques to delignify and isolate fiber from plant biomass. The dominant pulping process is the kraft process, which accounts for over 90% of chemical pulp in the world [5]. Conventionally, white liquor, a solution of sodium hydroxide and sodium sulfide, is mixed with wood chips in a heated pressure vessel known as a digester. Lignin in the wood chips reacts with the hydroxide and hydrosulfide anions to become alkali-soluble. This is accomplished by cleaving the aryl ether bonds in the phenolic units. The pulp product is removed and washed to be used in paper products, while the leftover black liquor is precipitated with acid to produce what is known as alkali lignin. Any remaining black liquor is recycled and used a fuel for the boiler operation for the digestor [6].

The organosolv process is a pulping technique that solubilizes lignin using an organic solvent at elevated temperatures. During this process, lignin is first chemically fragmented via the cleavage of aryl ether linkages in acidic or neutral acid-catalyzed systems. The degree of delignification is governed by pH and the solvent's ability to dissolve lignin fragments, participate in lignin fragmentation, and hinder condensation reactions [7]. Lignin is recovered via precipitation in water and subsequent filtration or centrifugation. This method can produce lignin at purity levels as high as 90% or more [8, 9]. Organosolv techniques provide advantages over the kraft process in that the lignin and solvent can be easily separated via distillation. The solvents are recovered and can be reused, and the lignin is recovered at higher quality. This results in a lower environmental impact, with less water pollution and a reduced odor compared with the kraft process.

Modifications

The complex and versatile structure of lignin provides the opportunity to use lignin in different applications. When direct incorporation of unmodified lignin cannot provide the desired properties, chemical modification can be employed to tune properties. Generally, these modifications are approached through two different strategies: lignin depolymerization and the creation of new chemical active sites [10]. Lignin depolymerization, or fragmentation, describes breaking down the lignin macromolecule into low molecular weight phenolic compounds. It has been the subject of years of research as a means to replace fossil feedstock in chemical synthesis

and has been achieved through many different processes including pyrolysis, hydrolysis, oxidation, gasification, hydrogenation, enzymatic oxidation, and microbial conversion [11, 12]. The synthesis of new chemical active sites is a strategy used to alter lignin functionality. Most commonly, hydroxyl groups are the target of these strategies, but there are other techniques being used, such as nitration, amination, alkylation, and hydroxylalkylation [10]. Functionalization of hydroxyl groups is the most common route as they are prevalent and reactive groups and therefore relatively easy to modify. Techniques for this include esterification, oxidative reduction, phenolation, and isocyanate reactions [13-16].

ADDITIVE MANUFACTURING

Types of Additive Manufacturing Processes

Additive manufacturing is the process of joining material layer-by-layer into a three-dimensional shape, typically under computer control. The layer-by-layer process allows for the fabrication of parts with more complex geometries than would be possible with comparable conventional manufacturing methods such as forging, machining, or molding. Because additive manufacturing (AD) techniques are usually computer controlled directly from a 3D model, the design and prototyping stage of product development are considerably quicker and more flexible. Because these technologies are additive rather than subtractive, they incur much less material waste and improve the product "buy-to-fly" ratio. Another benefit of using an additive technique is the potential to change or combine material during the build process [17]. This has led to faster and improved processing of polymer and metal matrix composites, which has been the focus of many recent studies [18, 19].

ASTM International lists seven process categories that describe current additive manufacturing techniques: binder jetting, directed energy deposition (DED), material extrusion, material jetting, powder bed fusion, sheet lamination, and vat polymerization [20]. The powder processes differ in joining method and material flow control. Binder jetting and powder bed fusion both use a bed of powder, but binder jetting joins the powders with a liquid bonding agent instead of the thermal fusion of powder bed fusion techniques like selective laser sintering (SLS). In contrast, DED processes thermally fuse powder as it is deposited. This group of technologies offer a potential wide range of material choices but is limited by the thermal and powder flow properties of the build material, which can cause incomplete fusion and porosity in the final part. Similarly,

material extrusion processes are also limited by material thermal and melt flow properties but are concerned with layer adhesion and print resolution as well. Sheet lamination processes combine additive and subtractive techniques by joining material in full layers and cutting each layer to the necessary shape. These technologies can use different binding and cutting methods, which result in a large material selection, but waste more material, have poorer resolution, and require more post processing than other AM processes. Material jetting and vat polymerization use light to solidify material but differ in that material jetting is a deposition technique and vat polymerization selectively adds from an excess quantity. Both benefit from high dimensional accuracy and material adhesion but are limited in material choice to specifically engineered photopolymer resins.

AM Market

The first commercially available 3D printing system debuted in 1987 with 3D Systems' SLA-1. In less than 5 years, material extrusion, sheet lamination, and powder fusion processes were developed and brought to market. Now, the value for worldwide AM products and services is expected to grow to $10.8 billion in 2021 [21]. This is largely due to the recent focus on research and development of AM processes by specific industries. Due to the advances in computer-aided design and systems control, the capability of AM processes to create accurate parts with desirable properties has improved. This has led to increased interest from industries such as the automotive, aerospace, and medical fields, who need the benefits offered by additive manufacturing. By 2025, the automotive, aerospace, and medical industries are expected to make up 51% of the AM market. More than any others, these fields have used additive manufacturing to improve product design and development. This includes rapid tooling for part testing and processing line optimization [22], complex topology optimization for light-weighting [23], and customizable parts for surgery and dental applications [24].

One major hurdle for all AM technologies is in designing new materials that are compatible with these AM processes but still comparable in cost and properties to those of traditional manufacturing. Many groups are researching and developing methods to bring existing, familiar materials to the AM space, but there has always existed an interest in novel materials and composites [25]. Renewable-sourced biomaterials are sustainable and potentially more environmentally friendly, giving them a competitive advantage over other conventional materials,

especially those derived from fossil fuels. As the technologies advance, there will be a greater demand for new materials that can accommodate a wider range of desirable properties. Engineering novel biomaterials provides the opportunity to develop materials that reduce the environmental impact of additive manufacturing while meeting traditional material requirements. However, meeting all these requirements presents a challenge where a balance must be made between material properties, processability, sustainability, and cost.

Stereolithography

Stereolithography (SLA) is widely used for applications where high precision is needed. Primarily, the healthcare industry is the primary user of SLA for medical, surgical, and dental modeling, as well as fabricating the implants themselves in some cases [24]. SLA processes use a UV laser to selectively cure a photopolymer resin in the standard layer-by-layer approach. To start, a 3D model is sliced into an image for each layer, depending on the layer height and the height of the model. The laser rasters the image onto the surface of the photopolymer resin vat. The first layers are cured directly on a build platform that moves through the vat, and all subsequent layers are cured onto previous layers. The layer height of the printed part is determined by the stepper motor on the build platform. The laser is controlled by a galvometer setup, which is what provides SLA with its high x-y dimensional accuracy.

In general, there are two configurations for stereolithography printers as shown in Figure 1: free surface and constrained surface [26]. In the free surface configuration, the laser is placed above the bath and the build platform is below the surface. Once the surface layer is cured, the platform lowers into the bath, and the next layer is cured. In contrast, the constrained surface configuration has the UV source below, emitting through a transparent bottom in the resin bath, and the build platform moving up out of the bath. The free surface configuration suffers from having the cure surface near air, which can lead to diffused oxygen scavenging radicals and a poorly cured part, whereas in the constrained surface configuration the resin vat provides an oxygen inhibition layer. However, the constrained surface configuration cures on the bottom surface of the resin tank, which can cloud and requires a peel cycle between each layer to remove the part from the resin tank without removing it from the build platform.

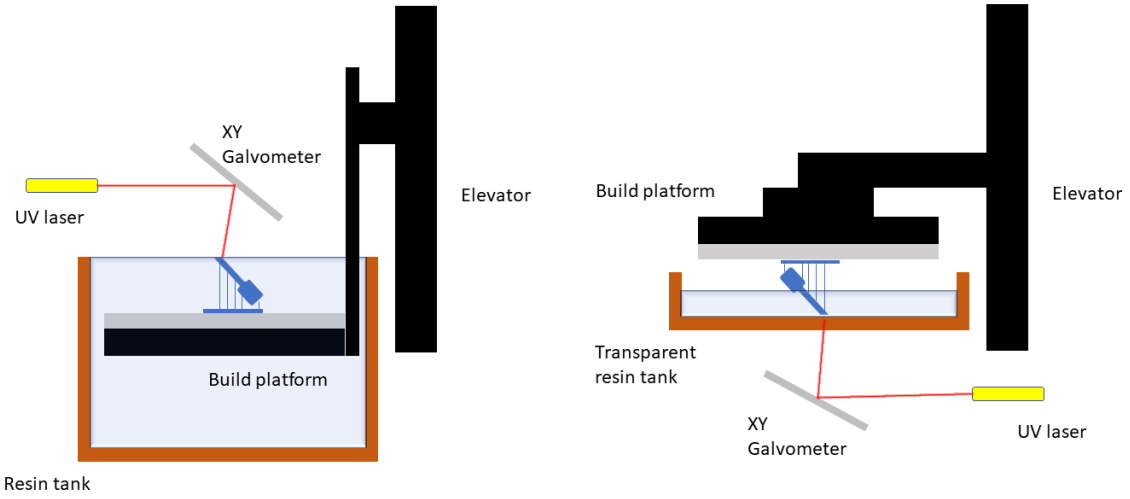

Figure 1. Standard configurations for stereolithography printers. In a free surface configuration, shown in the diagram on the left, the build platform is lowered into a resin bath. This limits the build volume by the depth of the resin tank. In a constrained surface configuration, shown in the diagram on the right, the build platform is raised out of the resin tank. In both cases, resolution control is decided by the step motor on the elevator and the mirror galvometer setup.

This process requires materials with carefully designed cure, rheological, and mechanical properties. The two fundamental cure properties of these resins are the penetration depth (D_p) and the critical cure dosage (E_c) [27]. These values are derived from the relationship between cure thickness (C_d) and applied dosage (E) based on the Beer-Lambert Law:

$$C_d = D_p \cdot \ln(E) - D_p \cdot \ln(E_c) \quad (1)$$

Choosing a cure thickness appropriate for the layer height, the required energy density for a resin can be calculated from this equation. The energy density can be tuned as part of the print parameters for the resin by controlling the laser power and speed. Precisely, the energy density is the laser power (P_L) over the scanned area per second, which is the product of the laser speed (V_s) and the scan line spacing (h_s):

$$E = \frac{P_L}{V_s h_s} \quad (2)$$

The penetration depth, defined as the depth of resin that reduces the irradiance level equal to 1/e that of the surface irradiance, and the critical cure dosage, the dosage required to begin

polymerization, are fundamental properties of the resin and therefore not controlled by print process parameters. They are determined by the components of the resin formulation interacting with light in range of the UV source.

PHOTOPOLYMERS

Standard photopolymers consist of monomers/oligomers, reactive diluents, and a photopackage, which is a photoinitiator (or suite of photoinitiators) and any necessary pigments, UV blockers, or sensitizers. There are two types of photoinitiators available for the purpose of polymerization: free radical photoinitiators and cationic photoinitiators [28]. For this reason, most photopolymers are either acrylate systems or epoxy systems. Free radical photoinitiators are ordered in two categories: type I photoinititators, which undergo a photofragmentation process, and type II photoinititators, which undergo a hydrogen atom abstraction process.

Since polyacrylates can be highly branched and crosslinked, these photopolymers tend to be brittle. A common strengthening strategy in photopolymer resins is to use polyurethane acrylates. These incorporate an alternating hard block-soft block structure in the polymer chain, which in turn creates a separated microstructure with amorphous soft polyol segments that provide mobility to the hard, crystalline segments [29].

CHARACTERIZATION

Lignin is an organic polymer with a complex and poorly understood structure. It is composed of different component monomers, guaiacyl, syringyl, and p-hydroxyphenyl, that combine through various linkages. The structure and composition change depending on the biomass source as well. Several characterization techniques can be used to obtain understanding of the effect of lignin and its modifications on material properties. These techniques inform on light absorption, structural configurations, functional groups, and thermal, mechanical and viscoelastic behaviors, and more. Analyzing the results of these characterization techniques is key to determining the efficacy of the modification and processing of these lignin materials.

UV-vis spectroscopy is a characterization technique that measures absorption or reflection in the ultraviolet and visible wavelength ranges of the electromagnetic spectrum. At these energies, molecules can absorb energy from light to transition between electronic states. By measuring the

change in light intensity, *I*, the absorbance can be calculated and used to relate the concentration *c* to a constant known as the molar absorptivity ε using the Beer-Lambert law:

$$\log_{10}\left(\frac{I_0}{I}\right) = A = \varepsilon c L \quad (3)$$

where L is the path length through the sample, generally 1 cm for most UV-vis cuvettes [30]. This is primarily used to quantitatively evaluate analytes, where the molar absorptivity is known, and a calibration curve can be generated. In Chapter 3, UV-vis spectroscopy is used to qualitatively determine the behavior of modified lignin in the UV wavelength range for curing of photopolymers.

Fourier-transform infrared (FTIR) spectroscopy is a related technique that measures absorption of light through a sample to detect the presence of specific compounds. This method differs in that it shines multi-frequency light through the sample repeatedly with changing frequencies, instead of a simple monochromatic light [31]. The collected data is then processed through a Fourier transform algorithm to separate out absorbance at each wavelength. Absorption data can be related to vibrations in the sample molecules which can be interpreted as structural characteristics that identify compounds.

Nuclear magnetic resonance (NMR) spectroscopy is another characterization method used to identify and evaluate chemical compounds. NMR exploits the phenomenon of nuclei response in an applied static strong magnetic field when exposed to an oscillating weak magnetic field [32]. The sample is placed into a magnetic field and excited into resonance, which is detected by radio receivers. The unique magnetic field around atoms in a molecule allow for detailed information on specific compounds and structures present to be determined. The modification of lignin is monitored using these methods to give insight to the changes in lignin's structure, which are then correlated to measured material properties.

Thermal gravimetric analysis (TGA) measures mass changes over time at different temperatures. It is a technique used to study chemical and physical phenomena such as thermal decomposition, oxidation and reduction, phase transitions, and chemical and physical absorption [33]. Measurements are taken using a high sensitivity mass balance in a furnace with programmable temperature control. Data are usually presented as percent mass versus temperature, often including the first derivative curve for comprehensive analysis. These data can be useful in

determining composition and thermal stability of materials. TGA is used in this work to measure changes to onset and peak decomposition temperatures in lignin acrylate polymers and evaluate the effect of lignin on thermal stability.

Mechanical properties such as elastic, or Young's, modulus, ultimate tensile strength, and percent elongation are obtainable with stress-strain curves, which can be generated using uniaxial tensile testing. Test specimen are prepared to a standardized specification that includes a gauge section of known cross-sectional area and grip shoulders designed to encourage failure in the gauge section. These specimens must be carefully made to avoid defects in the gauge section that can cause unwanted fracture behavior. Measurements are made to force and length, which are used to calculate stress and strain. Stress-strain curves can be used to calculate many mechanical properties as well as evaluate behavior such as if a material is brittle or elastic. These tests are applied to lignin acrylate polymers to quantify changes to stiffness, strength, and ductility owing to chemical modifications. It is assumed that the photopolymer materials tested in this study are isotropic even when printed due to the crosslinked structure persisting across layers [34].

Rheological behavior of materials is important to know in cases where processing conditions rely on predictable material flow. The choice of equipment and technique used to study this behavior depends on the property of interest. In this study, a rotational, or shear, rheometer in cone and plate geometry is used to measure viscosity. A cone with a known angle is placed on the sample material on a horizontal plate. Either the plate or the cone is rotated, and torque is measured on the cone. Shear stress is calculated using the torque response and degree of rotation, while the shear rate is given by the dimensions of the cone and the rotational speed [35]. Resins for 3D printing require precise flow behavior to operate properly in the apparatus used, so the effect of lignin on these properties is studied.

APPLICATIONS

Lignin is potentially applicable to many uses in polymer systems where UV and visible light absorption, transmittance, and scattering are important. UV degradation is a problem for most common polymers exposed to significant amounts of sunlight. Lignin is currently being researched as a low-cost filler to improve UV resistance in polymers composites and films [36, 37].

These properties are important to photopolymerizable systems, where UV protection is still a concern but must be controlled to allow for adequate cure conditions. These materials are commonly used in coating, adhesives, and sealants for a wide range of fields including medicine, dentistry, electronics, art, and construction. Many additive manufacturing processes use photopolymers including SLA, DLP, and material jetting. In each of these, precision is necessary in material cure and flow properties when designing a resin. Desired cure behavior is often achieved using a combination of components, so these industries are always interested in the development of new photoactive materials. Lignin has the potential to be valuable in these materials as it has been shown to be photoactive and versatile in properties through modifications.

The photoactive components of a specially engineered photopolymer are collectively known as the photopackage, and they consist generally of UV blockers, photoinitiators, and pigments. UV blockers are valued in transparent or nonpigmented resins for their ability to selectively absorb in UV wavelengths instead of the visible range. Lignin has potential here as it is partially transparent to visible light and could be used in applications where coloration is ignored. Because lignin primarily absorbs in low visible light wavelengths, it could be used in combination with other pigments to achieve specific colors while also offering UV protection. Little work has been done to study lignin as a photoinitiator, but depolymerization studies show that fractionation of lignin can produce low molecular weight chemical products with structures like commercial photoinitiators. Conceivably, lignin can be used to comprise the entire photopackage in some photopolymer applications.

Although lignin is widely used in polymers as a filler and additive, incorporation into a polymer network can be achieve through chemical functionalization. This has already been demonstrated with polyurethanes and polyphenols [15, 16]. Similar modifications through acylation allow for free radical polymerization of lignin. The versatility of lignin through processing means that various products such as prepolymers and crosslinking agents could be designed.

MOTIVATIONS AND OBJECTIVES

Although lignin is a potentially rich and abundant chemical source, efforts have yet to produce a clear, economically viable path toward valorization. Photopolymers are limited in composition and application, and lignin offers many advantages in the physical properties of the

polymer network and the cure properties during photopolymerization. Conventional applications for photopolymers, such as coatings and adhesives, might be able to employ a low-cost renewable material, but it is the niche but growing field of additive manufacturing that is poised take advantage of the unique properties of lignin in innovative manufacturing processes. This work addresses the modulation and application of these properties to these manufacturing techniques and resultant new materials.

Chapter 2 focuses on the modification of lignin to incorporate methacrylate groups in the structure of organosolv extracted hybrid poplar lignin, and the development of lignin-containing photopolymers for use in stereolithography. The primary objectives are to discover the barriers present in utilizing lignin in photoactive materials and to explore them with a resin formulation and processing approach. Lignin is modified and characterized with various spectroscopic techniques to monitor modification and evaluate structural changes. Resins are formulated with modified lignin and characterized to determine optimal cure properties that translate to process parameters on a commercial SLA printer. The resultant cured materials are characterized for mechanical and thermal properties and print quality.

Chapter 3 describes using various chemical modification techniques in the generation of prepolymer material to improve the cure properties of lignin acrylate resins. Absorption spectroscopy measurements were made to evaluate changes to the chromophoric structures in the modified lignin and determine which chemical strategies yielded usable material for photopolymers. Structural changes were further analyzed using FTIR and NMR spectroscopies and were correlated to thermal and mechanical characterization in resin materials. The results were used to determine the function of these modified lignin in photopolymer systems.

Chapter 4 recaps the main conclusions of this study as well as the significance of the work. A discussion is included on how these results can be applied and what additional efforts are necessary to continue the development of lignin-derived photopolymer materials.

CHAPTER 2

LIGNIN-CONTAINING PHOTOACTIVE RESINS FOR 3D PRINTING BY STEREOLITHOGRAPHY

ABSTRACT

Generating compatible and competitive materials that are environmentally sustainable and economically viable is paramount for the success of additive manufacturing using renewable materials. We report the successful application of renewable, modified lignin-containing photopolymer resins in a commercial stereolithography system. Resins were fabricated within operable ranges for viscosity and cure properties, using up to 15% modified lignin by weight. A 4-fold increase in ductility in cured parts with higher lignin concentration is noted compared to commercial stereolithography resins. Excellent print quality was seen in modified lignin resins, with good layer fusion, high surface definition, and visual clarity. These materials can be used to generate new products for additive manufacturing applications and help fill vacant material property spaces, where ductility, sustainability, and application costs are critical.

INTRODUCTION

Additive manufacturing offers greater freedom of design, quicker product development, and at a cheaper cost over traditional manufacturing techniques. In 2018, the global additive manufacturing (AM) market has a predicted value of $12.8 billion [21]. The complexity offered by greater design freedom means that parts can be topologically optimized to improve mechanical properties and hybrid materials can be designed that can achieve material properties unobtainable with conventional material processing [38, 39]. However, one major hurdle for all AM technologies is in the design of new materials that are compatible with these AM processes but still comparable in cost and properties to those of traditional manufacturing. Renewable-sourced biomaterials are sustainable and abundant, giving them a competitive advantage over materials derived from fossil fuels. Hence, engineering novel biomaterials provides the opportunity to create cost-effective materials that reduce the environmental impact of additive manufacturing while meeting traditional material requirements.

Stereolithography (SLA) is an AM process that uses a bath of liquid photopolymer resin, a movable platform, and a laser UV source to cure resin layer by layer to build part geometries. The main limitation of SLA technology is the photopolymer build material. In the next decade, the market for 3D printing materials is expected to grow to at least $16 billion, and a significant portion

of that is predicted to be shared by photopolymers [21]. Currently, these materials are few, limited in features, and expensive [40].

Resins designed for AM processes are complex mixtures generally composed of a photoinitiator, monomers and oligomers, and other additives incorporated to achieve specific properties. Photosensitizers and UV blockers, for instance, can be added to shift cure wavelength and affect reaction kinetics [41]. Resin formulations are finely tuned to work efficiently with the printer configuration and achieve the desired material properties. As expected, these complex formulations are costly to design and produce. In addition to cost, photopolymers typically exhibit issues with shrinkage, brittleness, and slow cure speed. In SLA, these problems are related to the photopolymerization reaction. Therefore, one approach to solving these problems is to control the reaction by altering the resin formulation.

Lignin is the world's second-most abundant natural polymer, and the only high-volume renewable feedstock composed of aromatics [42]. Most of the lignin available is produced as a byproduct of cellulose production, and although much of it is used as a fuel source for these processes, some methods can generate up to 60% more lignin than is used during combustion [43]. In fact, by 2022, 62 million tons of lignin will be produced annually [44]. Second-generation biofuels derived from lignocellulosic sources are poised to play an important role in alternative energy solutions, and the economic success of these biorefineries lies with co-product revenue streams.

Much work has gone toward the valorization of lignin for use in fuels and chemicals. Lignin also shows great promise for use in sustainable polymers and soft materials, and several commercially viable products containing lignin have been investigated [45, 46]. Recently, organosolv and aquasolv lignin have been used as additives in polymer composites, without prior functionalization, to enhance the structural rigidity [47, 48]. As demonstrated in these investigations, lignin-containing composites formed via injection molding or fused deposition molding (3D printing) exhibited improvements in interlayer adhesion and a corresponding increase in tensile strength. However, such improvements were achieved via noncovalent hydrogen bonding or physical cross-linking, and hence, additional reinforcement was required to improve the overall material toughness. Such limitations could be overcome by suitably modifying lignin such that it forms covalent linkages with the copolymer molecules.

In contrast to simply blending technical lignin with existing petrochemical-based polymers, chemical modifications to isolated technical lignin typically lead to improved chemical, physical, and thermal properties of the resulting product. In fact, these can even offer additional functionality, such as an increase in photoactivity. For instance, bio-plastics developed from acylated model-lignin compounds like syringol, creosol, and vanillin were shown to possess enhanced thermal stability and tunable viscoelastic properties [49, 50]. Bio-based epoxy resins made from depolymerized and glycidylated softwood lignin displayed superior flexural modulus and flexural strength [51]. Our group has also recently demonstrated that engineered hydrogels containing methacrylate-modified hardwood lignin exhibited increase in water retention capacity and tunable mechanical properties [52]. Moreover, alkene-functionalized lignin was successfully harnessed for photo-induced polymerization reactions [53]. In short, these studies demonstrate that designing lignin building blocks via chemical modification of the OH groups is a feasible approach for formulating 3D printing resins with tunable properties.

We are interested in developing transformations of lignin to make it amenable to incorporation into new high-performance engineered materials. Here, we report on our efforts to produce photoactive resins that contain organosolv lignin isolated from hybrid poplar. We formulated these resins by chemically modifying the lignin macromolecules to contain methacrylate moieties. Then, we blended the lignin with commercially available resin components to formulate a complete resin. We used a commercial desktop 3D printer from Formlabs to print with these resins, and report on the spectroscopic, mechanical, and thermal properties of these materials. This work represents a platform from which the design of advanced photoactive resins for additive manufacturing purposes can commence.

EXPERIMENTAL

Reagents and Materials

Lignin was isolated from pulp-grade wood chips of hybrid poplar (Populus trichocarpa × P. deltoides) using an ethanol organosolv technique as described by Bozell and coworkers [54]. Ethoxylated pentaerthritol tetraacrylate (SR494, Sartomer) and aliphatic urethane acrylate (Ebecryl 8210, Allnex) were used as resin bases. A monofunctional urethane acrylate (Genomer 1122, Rahn) was used as a reactive diluent. Diphenyl (2,4,6-trimethylbenzoyl) phosphine oxide (PL-TPO, Esstech) and 2,2’-(2,5-thiophenediyl)bis(5-tert-butylbenzoxazole) (Benetex OB Plus,

Scheme 1. Synthesis scheme for lignin-M using methacrylic anhydride.

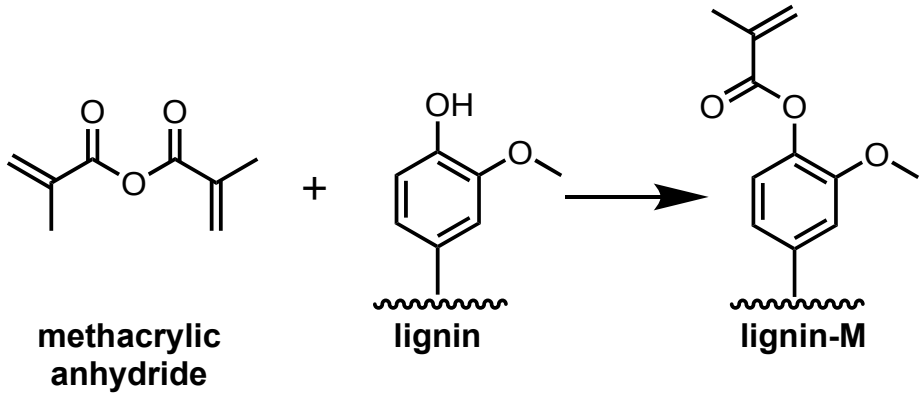

Mayzo) were used as the resin photoinitiator and UV blocker, respectively. Commercial PR48 resin was obtained from Colorado Photopolymer Solutions (Boulder, CO) for comparison purposes (the open-source recipe for PR48 is freely available online at the time of writing at https://learn.ember.autodesk.com/blog/open-sourceresin). 2-chloro-4,4,5,5-tetramethyl-1,3,2-dioxaphospholane (TMDP, Santa Cruz Biotechnology, Inc.) was stored in a vacuum desiccator to protect it from atmospheric moisture. Endo-N-hydroxy-5-norbornene-2,3-dicarboximide (Sigma-Aldrich) was used as received.

Lignin Modification for Resin Formulation

The protocol for lignin acylation (Figure 2) was adapted from the method for syringyl methacrylate synthesis as described by Epps and coworkers [49, 50]. Methacrylic anhydride (Alfa Aesar) was allowed to react with lignin (1.2 equiv of the lignin OH groups as measured by ^{31}P NMR) in the presence of 4-dimethylaminopyridine (DMAP, Sigma-Aldrich) as a catalyst (0.04 equiv of methacrylic anhydride). The reaction mixture was incubated at 60 °C for 48 hours and the lignin thus acylated (lignin-M) was purified by quenching the byproducts and unreacted substrate with a saturated solution of sodium bicarbonate. Lignin-M that precipitated during the reaction was washed with copious amounts of water until the washes reached neutral pH. The resulting precipitate was dried under reduced pressure at 40 °C for 48 hours and used for resin formulation.

Lignin Characterization

The hybrid poplar lignin and lignin-M were characterized using ^{31}P NMR and Fourier transform infrared (FTIR) spectroscopies to monitor the chemical changes in lignin and the efficiency of acylation reaction. Sample preparation and quantification of lignin OH groups was achieved using ^{31}P NMR spectroscopy as described by Balakshin and Capanema [55]. Briefly, the lignin samples were phosphitylated using TMDP, and the resulting NMR spectra were phased and referenced to the chemical shift of the water-derived complex of TMDP (δ 132.2 ppm). Quantification was achieved using endo-N-hydroxy-5-norbornene-2,3-dicarboximide as the internal standard. All ^{31}P NMR spectra were collected using a Varian 400-MR spectrometer (Varian Inc., Palo Alto, CA), operating at 161.92 MHz and 25 °C. FTIR spectra in the range of 4000 to 600 cm–1 were obtained using a UATR Spectrum Two instrument (PerkinElmer, Llantrisant, UK), where the finely ground samples were analyzed at 16 scans per spectrum and 4 cm-1 resolution. The FTIR peaks were assigned based on previous reports, and the spectra were subjected to statistical analysis using principal component analysis (PCA) [56-58].

Resin Formulation

The formulations of the 3-D printing resins used in this investigation are presented in Table 1. The photoinitiator and UV blocker were weighed and combined in a polypropylene container. The resin bases were added by weight in increasing viscosity as follows: the monofunctional urethane acrylate (Genomer 1122), the tetra-acrylate oligomer (SR494), and finally the aliphatic urethane acrylate (Ebecryl 8210). The partially formulated resin was mixed in a kinetic mixer (FlackTek, Speedmixer Dac 150 FVZ) at 2400 RPM for 0.5 min. Lignin-M was then weighed and added to the container and the resin was mixed again at 2400 RPM for 1 min. The lignin resins (LR) thus formulated (5-15% lignin by weight, LR5, LR10, and LR15) were stored in tightly sealed opaque containers to protect them from light.

Resin Working Curves

All resins were characterized for critical cure dosage and penetration depth parameters using the working curve method outlined elsewhere [27]. This method relies on a relationship between cure thickness and dosage derived from the Beer-Lambert Law as shown below:

$$C_d = D_p \cdot \ln(E) - D_p \cdot \ln(E_c) \quad (4)$$

Table 1. Composition of Modified Resins

Resin	SR494 (wt%)	Ebecryl 8210 (wt%)	Genomer 1122 (wt%)	Lignin-M (wt%)	PL-TPO (wt%)	Mayzo OB+ (wt%)
PR48	39.78	39.78	19.89	0	0.4	0.16
LR5	37.84	37.84	18.92	5	0.4	0
LR10	35.84	35.84	17.92	10	0.4	0
LR15	33.84	33.84	16.92	15	0.4	0

where C_d is the cure depth, D_p is the penetration depth, E_c is the critical dosage exposure required to cure the resin, and E is the dosage applied per layer. This dosage can be controlled by the laser scan velocity in accordance with the following relation:

$$E = \frac{P_L}{V_s h_s} \quad (5)$$

where Vs is the scan line velocity, hs is the scan line spacing, and PL is the laser power. Together, equations 5 and 6 can be used to experimentally determine D_p and E_c, since a plot of cure depth (thickness) versus the natural log of dosage (E) can be fit with a line whose slope is penetration depth (D_p) and whose y-intercept (b) is given as

$$b = -D_p \cdot \ln(E_c) \quad (6)$$

A rectangular model was designed using AutoCAD (Autodesk, Inc., San Rafael, CA) having dimensions 40 × 64 mm2. It was composed of 32 squares that had varying thickness ranging from 5 to 20 layers. The model was printed directly on the resin bath to ensure that the resultant thicknesses were due only to the applied dosage. Excess resin was used to avoid oxygen inhibition of curing during lazing. The 3D printed specimen was removed from the bath and cleaned of excess resin. The material thickness was measured for each square using a digital Vernier caliper and plotted against the natural log of the dosage. A linear regression was performed on the data to obtain the slope (corresponding to D_p) and y-intercept (related to the critical dosage as described by equation 3 above).

3D Printing Using Lignin Resins by Stereolithography

Models for 3D printing were designed in AutoCAD, and all samples were generated using a Formlabs (Formlabs, Inc., Somerville, MA) Form 1+ desktop stereolithography (SLA) printer,

installed with a modified version of the printer's software called OpenFL. The SLA printer used a 120 mW Class-1 laser emitting at 405 nm and had a build volume of 125 × 125 × 165 mm^3. The 3D printing resins were stored and used at room temperature. Custom print files were designed for PR48 and the LR resins using dose calculations obtained from the resin working curves. The laser settings for were obtained by modifying the laser-scan velocity that delivered the necessary dosage, as per eqn. (2). Print files were designed to cure the resins of 50 µm thickness. OpenFL was used to generate the scaffolds before printing. Tensile bars were built at a 45° angle with scaffolds edited to avoid placement along the gauge length.

The printed parts were separated from the build platform and soaked in two consecutive baths of isopropanol for 10 min each to remove any uncured resin and scaffolds. A 400 W metal halide UV (arc) lamp (Uvitron International Inc., West Springfield, MA), with irradiance capacity of 200 mW/cm^2 at a height of 7.62 cm was used to post-cure the printed parts for 3 min.

Materials Characterization

The viscosity of the formulated resins was measured using a TA Instruments AR-G2 rheometer with cone and plate geometry. The rheometer was configured with a 40 mm diameter cone at a truncation gap of 56 µm. Tests were performed over a range of shear rates from 0.1 to 100 Hz at 25 °C.

Chemical characterization of the cured samples was performed using FTIR spectroscopy, where the solids samples were directly analyzed on the crystal of an ATR accessory attachment. Five individual spectra were collected for all samples. Thermogravimetric analysis (TGA) was performed using a PerkinElmer Pyris 1 TGA. Each test was programmed to run from 30 °C to 900 °C at a heating rate of 20 °C/min. All tests were done under a continuous nitrogen flow of 10 mL/min.

Ultimate tensile strength and Young's modulus of the cured samples were obtained using an Instron 5567 dual column universal testing machine. A 30 kN static load cell was used. Tests were performed following the ASTM D638 standard according to type V specimen dimensions. A 1 mm/min extension rate was applied for all tests. Scaffold marks on printed samples were removed by sanding prior to testing to avoid any stress concentration.

Scanning electron microscopy (SEM) was performed using a Phenom ProX with an accelerating voltage of 10 kV. Samples were cut to size and cleaned of debris prior to mounting.

RESULTS AND DISCUSSION

Modified Lignin Characterization

Lignin-M, obtained via acylation of OH groups of hybrid poplar lignin with methacrylic anhydride (Scheme 1), was characterized using ^{31}P NMR and FTIR spectroscopy. Figure 3a depicts the FTIR spectra, in which lignin-M had a significant reduction in OH functional groups (3403 cm-1). This is expected, as the number of OH groups is depleted as the acylation reaction takes place (Scheme 1). The FTIR spectra indicate an increase in methacrylate functional groups attached to the modified lignin OH groups, as evidenced by increases in peaks corresponding to C=O stretches, C-O-C stretches, and in plane –CH2 bending vibrations (1723, 1131 and 943 cm-1, respectively).

^{31}P NMR spectroscopy is another method used to quantify the changes in lignin OH groups and is particularly useful to detect differences among substitution at the aliphatic, syringyl (S), guaiacyl (G), para-hydroxy (H), and carboxylic acid (COOH) hydroxyl groups. As shown in Figure 3b, OH groups in lignin-M undergo substantial substitution, where 92% of these are acylated. The scant amounts of COOH groups (0.1 mmol/g) observed in lignin-M might have originated from residual methacrylic acid, which is a byproduct of lignin modification.

LR Formulations

We used lignin-M as a source of acrylate oligomers and reactive diluent at 5 to 15% by weight to formulate our 3D printing resins. To ensure that lignin-M was incorporated into the resin bases homogenously, we created the LR mixtures in small batches and allowed them to rest for 48 h. Unmodified lignin dissolved poorly in acrylate-based resins, whereas lignin-M showed significant improvement in homogeneity owing to the compatibility of its methacrylate functional groups (Figure S1).

We identified resin viscosity as a critical parameter for compatibility with an additive printing mechanism because of its role in affecting the resin recoating procedure over the curing surfaces between two contiguous layers. Fast laser scan speeds meant that, in general, the speed at

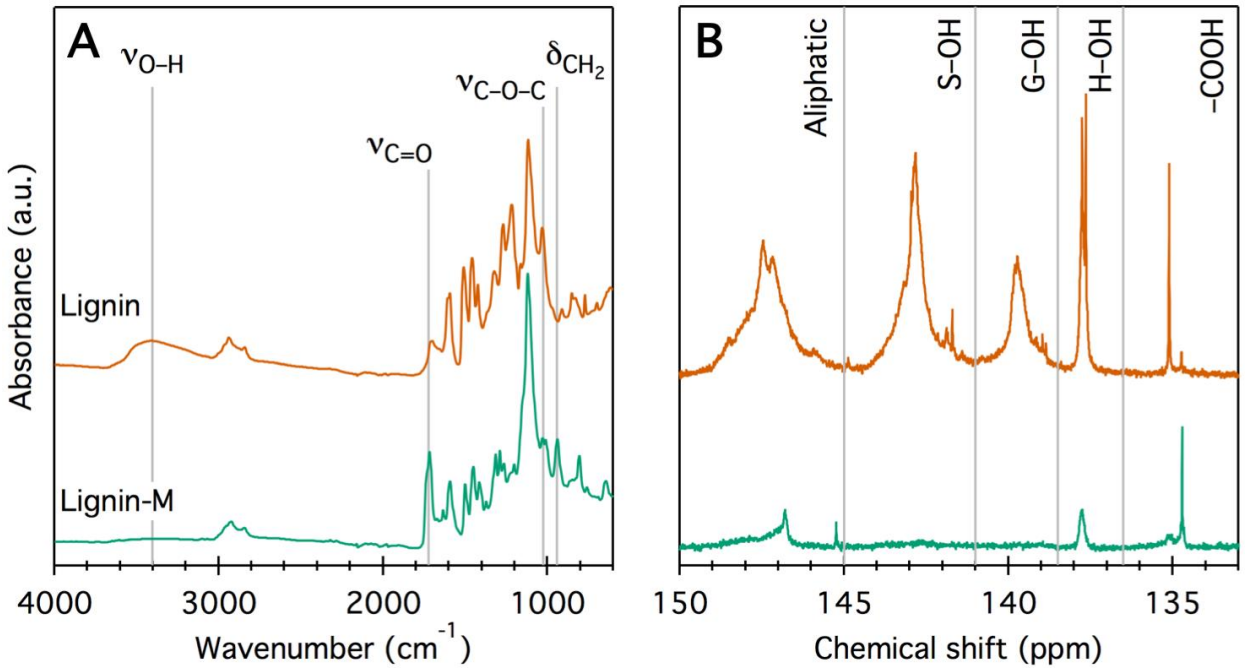

Figure 2. (A) Fourier transform infrared spectra of hybrid poplar lignin before (top, brown) and after (bottom, green) methacrylate modification of the OH groups to afford lignin-M. (B) 31P NMR spectra of the same samples (color scheme and position identical) with integration ranges taken from Balakshin and Capanema [55].

which the part can be printed is determined by how quickly the printer can reset for a new layer. Higher viscosities result in longer wait times for the recoating procedure and overall longer printing duration. The viscosity measurements for LR5-15 (Figure 4) showed that they displayed Newtonian behavior and had a viscosity range from 0.44 to 1.66 Pa·s. Commercial manufacturers have reported viscosities in the ranges of 0.85 to 4.5 Pa·s for their 3D printing resins, so LR5-15 are evidently viable for creating equivalent print designs. The measured viscosity of LR5-15 increased with increasing lignin-M content, which implies a limit to the amount of lignin the base resin can host and still be within a usable viscosity range without additional diluent.

Resin Cure Properties

The working curve approach is a basic model for formulating SLA resins, since it provides a measurement of threshold energy required to initiate photopolymerization (E_{crit}) and also helps to evaluate the resin cure properties [27]. The working curves generated for all LR formulations are shown in Figure 5, and the corresponding cure properties are listed in Table 2, along with the target dosage for a printing a layer with a thickness of 50 μm (a photograph of the windowpane rectangle used to generate working curves is provided as Figure S2).

Penetration depth (D_p) is the distance photons travel in the resin before they are absorbed by a resin component. Resins with high D_p will allow more photons to pass farther into the resin, causing it to potentially cure thicker than a resin with a lower D_p. This results in poor resolution control and nonuniformity in the build geometry. Typically, SLA resins contain a UV blocker (Mayzo OB+ in PR48, see Table 1) to tune the D_p and reduce the required precision during printing.

Since lignin contains several UV-active moieties (aromatic rings and C=O bonds), we expected that it would readily absorb UV photons and potentially serve the same role as the UV blocker. Consequently, we prepared all LR formulations without Mayzo OB+. Surprisingly, the added lignin does not appear to retard the penetration of the UV photons to the same degree as the UV blocker in PR48. As is evident from the data in Table 2, even up to 15 wt-% lignin-M, D_p for the LR formulations was still higher than that for PR48, which contains 0.16 wt-% UV blocker. As expected, D_p decreased in resins with higher amounts of incorporated lignin-M. Evidently, lignin-M in the LR resins could act not only as a structural feature but also as a UV blocker, albeit

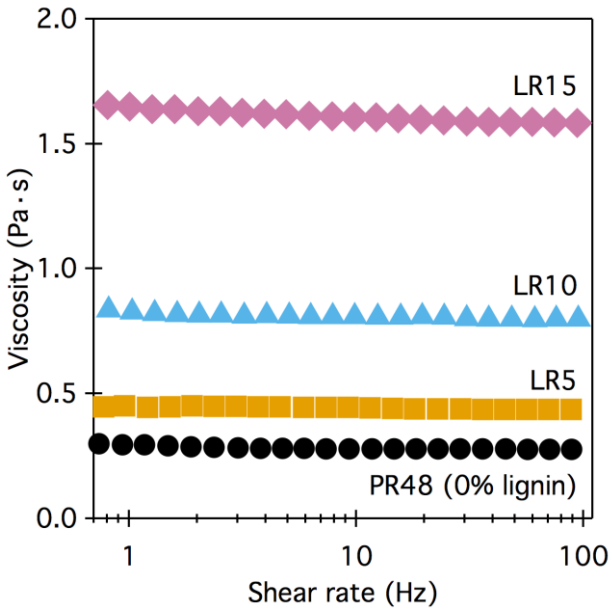

Figure 3. Plot of viscosity versus shear rate of photo curable acrylate resins containing various amounts of lignin-M. Viscosity increases with increasing amounts of lignin as compared to the commercial PR48 resin.

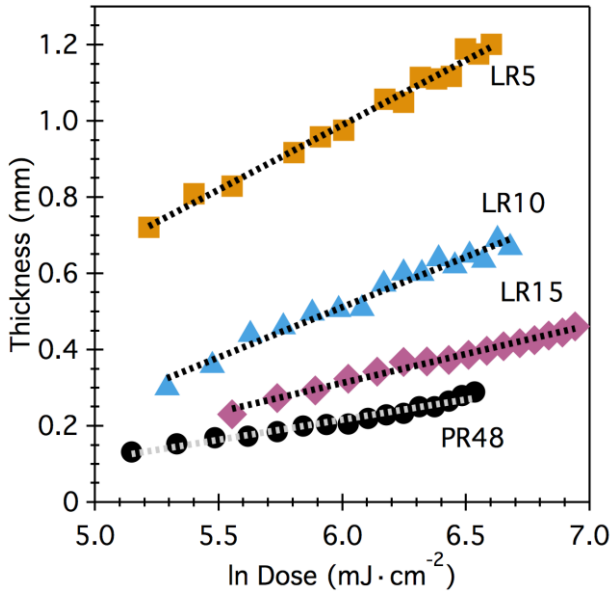

Figure 4. Working curves showing cure thickness as a function of the natural log of UV dosage for PR48 and LR formulations. Linear regressions are shown as dotted lines, and the related values are tabulated in Table 2 from Equations 1-3 above.

with much lower efficiency compared to traditional UV blockers. We are currently investigating the efficacy of lignin to be used as a specialized UV blocker in these formulations

Interestingly, the critical cure dosage (E_c) decreases significantly in at 5-wt% loading but changes little for higher amounts. Although a higher critical cure dosage will result in a larger starting dosage and could significantly increase the curing time, evidently the presence of lignin does not deter resin curing. However, since the LR formulations do not include a UV blocker, the presence of which would increase the critical cure dosage, we are unable to unambiguously determine the reason for the change in E_c. We hypothesize that the complex lignin structure is beneficial in some parts to forming radicals for polymerization and detrimental in other, since lignin is known to be excited by UV light and quench the free radicals by undergoing redox reactions resulting in the formation of quinones [59]. There is certainly a complex interplay between penetration depth and critical cure dosage that depends upon the amount of lignin in each sample. We are currently investigating these phenomena further.

Characterization of 3D Printed and Cured Resins

We used FTIR spectroscopy of the polymerized resins and analysis of FTIR spectra (Figure S3) by PCA to probe the chemical structure of the cured resins. From these, we determined that the lignin-M containing polymers were significantly different than the control (Figure 6a).

As indicated by the PC1 loadings plot (Figure 6b), the largest difference between PR48 and the LR formulations is due to the presence of unconjugated carbonyl bonds (C=O), acrylate ester bonds (C-O-C) and in-plane bending of C=C groups (1723, 1191, and 1407 cm-1, respectively) in PR48. These can be attributed to unreacted acrylate groups in PR48 due to an

Table 2. Cure parameters for tested resin formulations

Resin Formulation	D_p (mm)	E_c ($J \cdot cm^{-2}$)
PR48	0.105(5)	0.05(2)
LR5	0.34(1)	0.022(5)
LR10	0.26(1)	0.06(2)
LR15	0.152(5)	0.05(1)

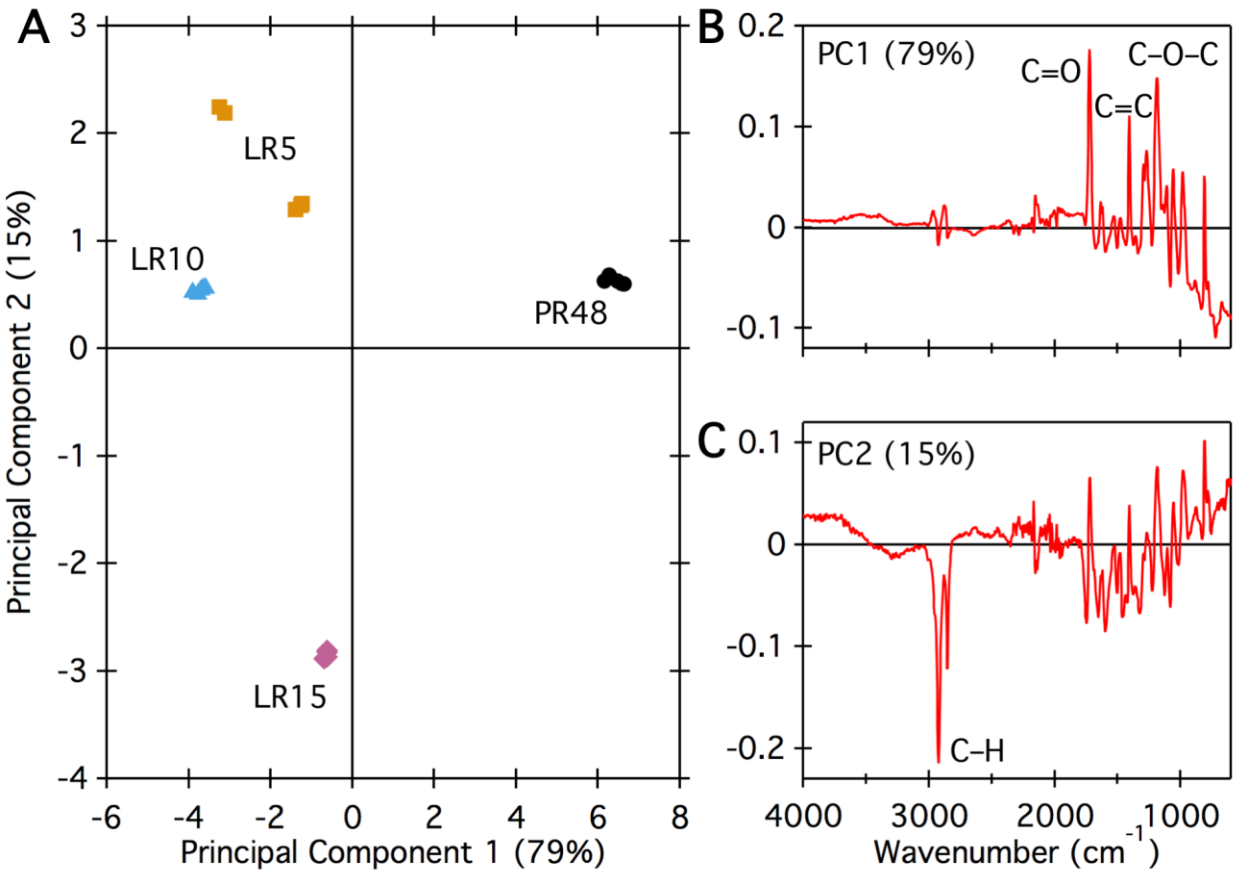

Figure 5. (A) Scores plot of the principal component analysis (PCA) of the FTIR spectra of printed and cured PR48, LR5, LR10, and LR15 resin formulations. The labeling scheme is identical to Figure 2. (B) Loadings plot of principal component 1 (PC1), which accounts for 79% of the data variance. Stretching frequencies for C=O, C=C, and C–O–C moieties are noted. (C) Loadings plot of PC2, which accounts for 15% of the data variance. Stretching frequencies for C–H moieties are noted.

incomplete cure. We further observed these results from scanning electron micrographs (vide infra) which we attribute to sub-optimal printing parameters (see Figure 8). This suggests that the LR formulations achieved a higher cure conversion than the commercial PR48 formulation using the printing parameters we selected. These printing parameters were chosen based the model in eqn. (1). It is possible that light scattering by the included UV blocker makes this a poor model for evaluating cure properties in PR48. Additionally, the PC2 loadings plot (Figure 6c) indicates that LR15 displayed higher asymmetric and symmetric stretching vibrations of C–H bonds (at 2923 and 2855 cm-1, respectively). This could possibly be attributed to the additional aliphatic groups in lignin, although this difference between the resins is relatively minor as reflected by the low percentage of contribution to the data variance (15%).

We performed tensile tests on the cured resins, and the results of these experiments are summarized in Table 3. Interestingly, the cured resins displayed a transition from brittle to ductile behavior in those that contain lignin-M. The elastic modulus showed a 43% decrease from 0.65 GPa with no lignin to 0.37 GPa with 15% lignin-M. Likewise, the ductility increased from a measured 1.87% elongation at break for the control to 7.62% for LR15. This indicated that lignin-M was acting as a plasticizer in the resin system. We attribute this phenomenon to the fact that the modified lignin molecules were introducing side chains in the polyacrylate that reduced the chain-to-chain interaction forces [60]. The decrease in elastic modulus in the LR formulations is likely a result of reduced cross-linking density due to these side chains. Photopolymers are usually brittle because of high cross-linking, so formulations tuned to inhibit this are a common strategy to improve toughness. This data suggests lignin could prove useful in these applications. However, further work needs to be done to increase the imparted stiffness before lignin is competitive with conventional materials.

We used thermogravimetric analysis (TGA) of the printed and cured resins to study the thermal properties of these materials. TGA data (Figure 7) demonstrate that the cured LR resins exhibited different degradation onset temperatures when compared to the control. The mechanism of thermal decomposition of cured polyacrylate resins such as PR48 and the related LR formulations has been the focus of intense investigation by several groups. The rate of thermal decomposition of PR48 accelerates as the temperature increases as evident by the first derivative of the TG curve. This phenomenon is known to be due to a complex combination of kinetically

Table 3. Mechanical testing of molded resins

Resin	E (GPa)	σ_R (MPa)	ε_R (%)
PR48	0.65(5)	11.0(4)	1.87(8)
LR5	0.64(2)	11(1)	3.0(1)
LR10	0.48(2)	18(3)	6(1)
LR15	0.37(2)	15(8)	7.6(1)

Relative uncertainties in the final digit are reported in parentheses.
E: tensile modulus; σ_R: failure stress; ε_R: strain at break

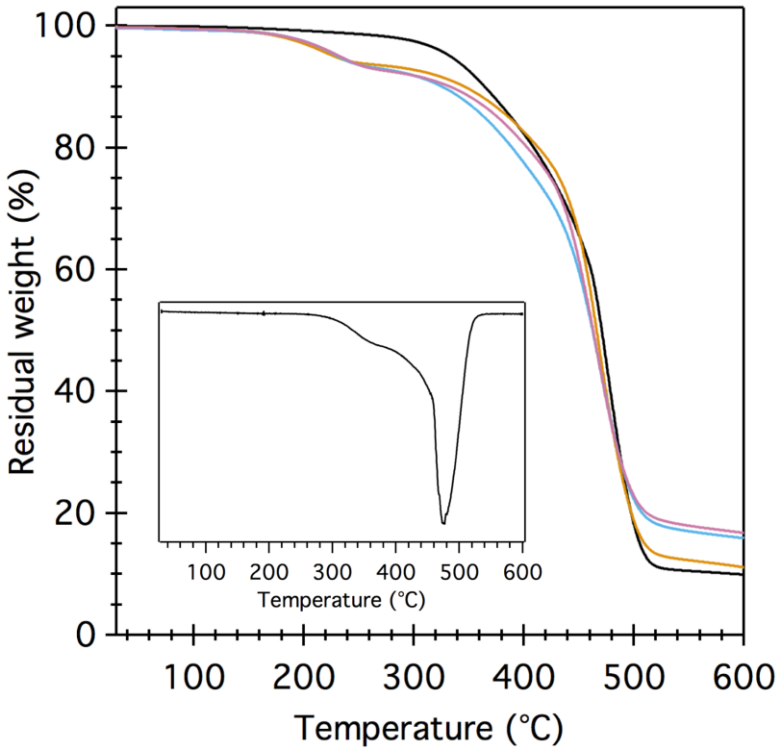

Figure 6. TGA curves (color scheme identical to Figure 4) for 3D printed commercial PR48 resin and LR formulations. The derivative of the weight curve (inset) demonstrates the change in rate of thermal decomposition of PR48. The decomposition of the LR formulations at ~185 °C is evidence of thermolysis of the ether bonds that link lignin-M to the poly(acrylate) backbone.

regulated chain scission and depolymerization reactions [20]. In case of the cured LR formulations, we attribute the small weight loss at about 185 °C to scission of the ether bonds that link lignin-M to the growing polyacrylate polymer and the related decomposition of the lignin-M oligomers, owing to the enhanced lability of C–O bonds in comparison to C–C bonds [61].

Morphology and Print Quality

We used scanning electron microscopy to characterize the 3D printed surfaces (Figure 8). The surface of cured PR48 showed significant gaps between layers, due to a lack of fusion between them. These defects were regularly aligned along the edges of the line scan width where the dosage will be at minimum, whereas the fusion at the center of the cross-line scans extended between the layers. Since the print did not fail on the build platform, we attribute this phenomenon to a higher required UV dosage to attain inter-layer adhesion in PR48. Evidently, at the print settings we have chosen for this study, optimal addition of lignin-M could enhance the photo-reactivity of the acrylate resins, thereby producing better prints at lower UV dosages.

LR5 provided the best print quality with relatively smooth surfaces and excellent layer adhesion, despite printing with the fastest laser scan velocity and at the lowest dosage. Print surfaces for LR10 and LR15 had small regions of poor fusion along print lines. These voids tended to be grouped together, suggesting that the presence of lignin-M disrupted the assemblage of polyacrylates due to cross-linking with lignin. Excepting these small regions, the surfaces of the 3D printed LR formulations showed complete fusion between layers, which emphasizes not only that lignin-M is compatible with SLA technology at the print layer level, but also that lignin-M shows great potential as a binding agent for improved print quality.

Visual evaluation of the print quality showed that the LR formulations displayed good build geometries compared to that of the commercial resin (Figure 9). High resolution and edge definition are achieved with the designed print settings. A significant degree of curling is present in the cured LR5 print because of the fast cure rate. Faster cure rates generally result in uneven shrinkage, causing a build-up of residual stresses and deformation of the material. Shrinkage can be reduced in this case either by modifying the resin formulation such that it has better optimized cure properties for this resolution or by changing the post-cure process. We did not observe this problem in the slower curing LR10 print in comparison to PR48, so we conclude that the added lignin is not significantly contributing to shrinkage beyond its effect on cure rate. Transparency

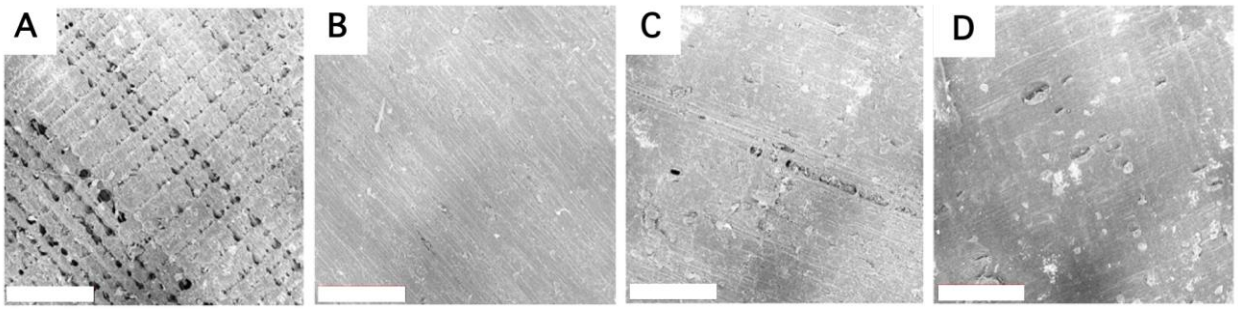

Figure 7. SEM images of the print surfaces for PR48 (A), LR5 (B), LR10 (C), and LR15 (D) showing an increase in surface roughness for LR formulations. Scale bars (white rectangles) denote 300 μm.

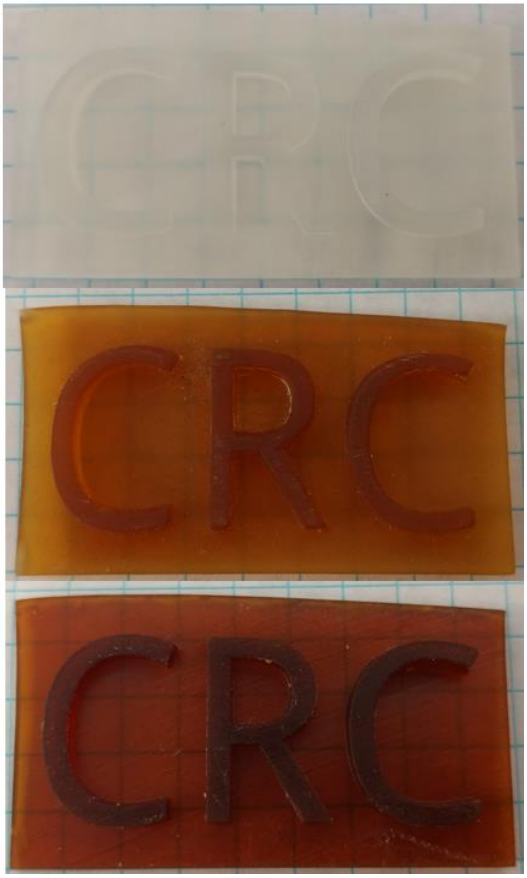

Figure 8. Photographs of 0% (PR48, top), 5% (LR5, middle), and 10% (LR10, bottom) lignin showing the effect on print quality. Even lignin-containing samples show translucence, suggesting they are amenable to pigmentation.

was reduced with higher amounts of lignin-M, but the resins did not cure fully opaque. Thus, pigmentation could be applied to change the resin color, however, the brown coloration of lignin may limit the range of colors that could be used successfully.

CONCLUSIONS

In this work, we generated new photo-active acrylate resins by mixing commercially available resin components with acylated organosolv lignin. The resulting mixtures contained up to 15% by weight lignin and were used to produce 3D prints via SLA technology. The lignin-containing resin formulations exhibited increased ductility but decreased thermal stability when compared to the commercially available control resin. Overall, we used the LR formulations to generate uniformly fused, high-resolution prints that display enhanced material toughness with a lower UV dosage. Future work will focus on investigating the role that lignin plays as a UV blocker in these resin formulations and using strategies to link functional monomers to lignin using C–C bonds instead of thermally labile C–O bonds.

ACKNOWLEDGMENTS

This project was supported by funds from the University of Tennessee AgResearch Innovation Fund. Additional funds were provided by the Southeastern Sun Grant Center and the US Department of Transportation, Research and Innovative Technology Administration DTOS59-07-G-00050. D.P.H. and S.C.C. also acknowledge support from the USDA National Institute of Food and Agriculture, Hatch Project 1012359.

CHAPTER 3

LIGNIN MODIFICATION TO IMPROVE UV CURING IN PHOTOPOLYMERS FOR STEREOLITHOGRAPHY

"This is a draft version of the following article: Jordan T. Sutton, Kalavathy Rajan, David P. Harper, and Stephen C. Chmely (2019) Lignin Modification to Improve UV Curing in Photopolymers for Stereolithography, which is in the process of publication."

ABSTRACT

Despite recent successes incorporating lignin into photoactive resins, lignin photo-properties can be detrimental to the application of lignin to UV-curable photopolymers, especially to specialized, engineered resins for use in stereolithography printing. We report on chemical modification techniques employed to reduce UV absorption in lignin and the resulting mechanical, thermal, and cure properties in these lignin materials. Lignin was modified using acylation and reduction reactions and incorporated into a printable resin formulation. UV absorption at the printing UV range was reduced in all modified lignin compared to unmodified from 25% up to greater than 60%. Resins made with the modified lignin show increased stiffness and strength with lower thermal stability. Studying these techniques is an important step in developing lignin for use in UV-curing applications and further the effort to valorize lignin toward commercial use.

INTRODUCTION

With the global emphasis on environmentally and economically secure industries, the search for high-value lignin-containing products continues at a quick pace. The core target products include fuels, chemicals, and polymers, and much work has been done to study lignin applicability in these areas [62]. Often these studies leverage intrinsic properties of lignin in targeting which products have the most promise, such as high phenolic content to replace the petroleum derived compounds in adhesives, redox behavior of lignosulfonates as electrolytes in flow batteries, and relatively high thermal degradation temperature to provide thermal protection to polymer composites [63-65]. In addition, research has been directed toward the photoactivity of lignin to design UV-resistant polymers, and lignin has even been studied as a UV blocker for broad-spectrum sunscreen formulations [66-70]. Perhaps unsurprisingly, developing lignin-containing photopolymers has attracted much less attention, probably due to the perceived hurdle of lignin blocking light in the UVA and UVB ranges, which are common curing ranges for photopolymers.

Lignin is the second most abundant natural polymer beside cellulose, and it is the most abundant renewable aromatic feedstock [2]. As such, it has high potential for application in the chemical and pharmaceutical industries. Lignin depolymerization is a topic of growing interest which encompasses isolating and using high-purity, low molecular weight products [68]. However, most of the lignin available today is supplied by the Kraft pulping process as a byproduct of cellulose production, and most Kraft lignin is sulfonated and generally requires purification before use [6, 71]. Higher quality lignin can be obtained through other extraction techniques such as any of the several solvent-based fractionation processes [37, 72]. These also offer the advantage of being more environmentally friendly through reduction of hazardous waste [73]. However, with any extraction process, the structure of the resulting lignin will be altered from its natural form [74].

Lignin is composed of phenylpropane groups arranged in complex inhomogeneous network structures that vary based on the plant species. Like any polymer, these structures give lignin its unique properties; however, the structural heterogeneity of technical lignins render elucidating structure-property relationships extremely challenging. For this reason, applying lignin to a product for a specific desired result remains a Grand Challenge of 21st-Century biorefining. Nevertheless, these rich, complex structures also provide the possibility for chemical modifications that can tune its properties for more efficient use, and the synthesis of new chemical active sites on lignin is a topic that has been studied for many years [10]. Overall, these modifications have shown useful for improving lignin compatibility with polymers and polymer blends [75, 76].

Photopolymer materials are commonly used in adhesives, sealants, and coatings, and an emerging application of photopolymers that has significant economic impact is in additive manufacturing (AM) [77]. Stereolithography (SLA) is an AM process utilizing photopolymers that suffers from a lack of variety in material choice. Despite the challenges associated with lignin photopolymers, lignin-containing SLA resins could offer an environmentally-friendly option in a group of petroleum-derived, generally toxic materials [78]. Lignin has recently been applied to stereolithography with some success [79, 80]. Our group has previously shown that lignin can be used in commercially available SLA products to generate 3D printable lignin materials [81]. However, the reduced UV transparency imparted by lignin was a barrier to printing with increasing lignin loading amounts.

Accordingly, we report here our efforts to modify an organosolv lignin to reduce its inhibitive effect in photopolymer cure properties. We chose softwood pine lignin because it is an industrially relevant biorefinery energy crop in the United States [82]. We employed chemical modifications to introduce methacrylate or acrylate moieties onto the lignin macromolecule. In addition, we used chemical reduction with $NaBH_4$ to decrease photoactive moieties in an effort to enhance the photochemical reactions occurring in the presence of lignin that are relevant to SLA. We then blended the modified lignin in a base resin formulation to produce an SLA photopolymer resin. We performed characterization of the spectroscopic, mechanical, and thermal properties of all the samples. Finally, we used a commercial desktop 3D printer to print with these resins and evaluate print quality.

EXPERIMENTAL

Reagents and Materials

Lignin was isolated from southern yellow pine (*Pinus spp*.) using an ethanol organosolv technique reported previously [54]. Methacrylic anhydride (Alfa Aesar), acrylic anhydride (Accela), sodium borohydride (Acros Organics), sodium bicarbonate (Fisher Chemical), and dimethylamino pyridine (DMAP, Acros Organics) were used as received. Solvents, including N,N-dimethylformamide (DMF, Fisher Chemical), dimethyl sulfoxide (DMSO, Sigma-Aldrich) and tetrahydrofuran (THF, Fisher Chemical) were used during modification and characterization of lignin. An aliphatic urethane triacrylate (Ebecryl 284 N, Allnex Netherlands BV) was used as the resin oligomer base. The diacrylic monomer 1,6-hexanediol diacrylate (HDODA, UBC Chemicals) was used as the reactive diluent. The photopackage components consist of diphenyl(2,4,6-trimethylbenzoyl)phosphine oxide (PL-TPO, Esstech Inc.) as the photoinitiator and titanium dioxide (white) and pyrolyzed lignin (black) as pigments [83]. Commercial resins Rigid, Grey Pro, and Clear V2 were obtained from Formlabs (Somerville, MA) for determining print parameters. 2-chloro-4,4,5,5-tetramethyl-1,3,2-dioxaphospholane (TMDP, Santa Cruz Biotechnology, Inc.) was stored in a vacuum desiccator to protect it from ambient moisture. Endo-*N*-hydroxy-5-norbornene-2,3-dicarboximide (Sigma-Aldrich) was used as received.

Lignin Reduction

Lignin reduction was performed by reaction with sodium borohydride (100 wt%) in methanol for 2 hours at ambient. The resulting suspension was concentrated using a rotary evaporator, and the afforded solid was washed with deionized water over qualitative filter paper. The resulting lignin samples were dried under reduced pressure at 80 °C for 18 hours.

Lignin Acylation

We used a procedure for lignin acylation that we have reported previously, which is an adaptation of the method for syringyl methacrylate synthesis reported by Epps *et al* [49, 52, 81]. Briefly, one of either methacrylic anhydride or acrylic anhydride were allowed to react with lignin (1 equiv of the lignin OH groups as measured by ^{31}P NMR spectroscopy) in the presence of a catalytic amount of DMAP (0.038 equiv of anhydride) in DMF. The mixture was allowed to react at 60 °C for 48 hours. Acylated lignin was recovered from the solution by quenching with a saturated solution of sodium bicarbonate. The precipitated lignin was recovered, washed with water until the pH of the washes measured neutral, and dried under reduced pressure for 48 hours at 50 °C.

Lignin Characterization

All of the lignin samples were thoroughly characterized before and after each of the chemical modifications. To measure OH group content, lignin samples were phosphitylated using TMDP, and ^{31}P spectra were collected using a Varian 400-MR spectrometer (Varian Inc., Palo Alto, CA) operating at 161.92 MHz and 25 °C [32]. NMR spectra were quantified using endo-*N*-hydroxy-5-norbornene-2,3-dicarboximide as an internal standard, and the spectra were referenced to the water-derived complex of TMDP (δ 132.2 ppm).

FTIR spectra (4000-600 cm^{-1}) were collected using a UATR Spectrum Two instrument (PerkinElmer, Llantrisant, U.K.); samples were finely ground and analyzed using 16 scans per spectrum and 4 cm^{-1} resolution. The FTIR peaks were assigned based on previous reports [56-58]. Samples were prepared for UV-vis measurements by dissolution of lignin in dimethyl sulfoxide (DMSO) at a concentration of 1.0 g/L. Spectra were collected over the range of 200-800 nm using a Genesys 10s UV-vis spectrophotometer (Thermo Fisher, Waltham, MA).

Lignin molecular weight (MW) analyses were performed using a Tosoh EcoSEC gel permeation chromatography (GPC) system equipped with a refractive index (RI) detector. Samples were prepared in a 0.75 g lignin/1 mL THF solution with no additional pretreatment required due to the presence of acrylate and methacrylate groups on lignin. Measurements were calibrated using PMMA (500 – 1.0×10^6 Da) and collected at 25 °C.

Resin Formulation

A base resin was formulated to match closely in mechanical and cure properties to the commercial resins obtained from Formlabs. The base resin is composed of 40% reactive diluent (HDODA), 59% resin base oligomer (Ebecryl 284 N), and 1% photopackage. The photopackage consisted of 0.84% by total resin weight of photoinitiator (PL-TPO) and 0.16% by total resin weight pigment, equal parts black and white (lignin carbon and TiO_2 respectively). Instead of pigment, lignin-containing resins contained additional photoinitiator and substituted 5% lignin in place of oligomer. Resin components were mixed in polypropylene jars. Lignin, photoinitiator, and pigments were allowed to dissolve in the reactive diluent for 24 hours before mixing in the oligomer to ensure full incorporation. The components were premixed in a kinetic mixer (FlackTek, Speedmixer Dac 150 FVZ) at 1000 rpm for 1 minute as a wetting step and then mixed again at 1500 rpm for 1 minute. All complete resin mixtures were stored in sealed opaque containers to avoid unwanted reaction in ambient light.

Uncured resins were measured for viscosity and cure properties. Viscosity was measured using a TA Instruments AR-G2 rheometer. The instrument was configured in a cone and plate geometry with a 40 mm diameter cone at a truncation gap of 56 microns. Shear rate was measured over a range of 0.1 to 1000 Hz in ambient lab conditions.

Resin cure properties were characterized by the print parameters penetration depth (D_p) and critical cure dosage (E_c) to evaluate printability. The penetration depth is defined at the depth at which irradiance is reduced to 1/e the level at the surface. Critical cure dosage is defined as the exposure corresponding to the transition from liquid phase to solid phase at the gel point. The method for determining these parameters was first established by Jacobs and coworkers and is described more fully in our previous study [27, 81]. Briefly, squares are cured on a quartz glass substrate at various dosages and then measured for thickness. Cure thickness and the log of dosage

are linearly related, where the slope of the line relates to the penetration depth and the intercept relates to the critical cure dosage.

Cure Scheme and Material Characterization

Resins were cast between 15 by 15 cm quartz glass sheets separated at 1 mm. A controlled cure scheme was chosen to avoid cracking and voids incurred by excessive shrinking. The resins were cured for 20 minutes in a 10 W 395-400 nm UV cure chamber and then transferred to a 400 W metal halide UV lamp (Uvitron International Inc., West Springfield, MA) for 1 hour. The resin sheets were inverted halfway through each step. Resin sheets were removed from the glass and laser cut to tensile bars according to ASTM D638 type V dimension.

Ultimate tensile strength, Young's modulus, and elongation at fracture were determined for all resins on an Instron 5567 dual column universal testing machine using a 500 N static load cell. All tests were performed according to ASTM D638 standard procedure. A 1 mm/min extension rate was used for all samples, as well as a preload force of 5 N. All samples were sanded, cleaned, and evaluated prior to testing for voids, cracks, or any other sources of stress concentration.

RESULTS AND DISCUSSION

We showed previously that lignin can be used to make working SLA resins in commercial printer and resin systems [81]. However, at higher lignin loadings, UV penetration depth through the resins decreases significantly, requiring higher cure dosages and limiting the potential lignin content based on the capabilities of the printer. The reduction in UV penetration can be attributed to light absorption by chromophoric systems in lignin [84]. Reductions using $NaBH_4$ have been shown to disrupt these chromophores and decrease absorption, especially in the wavelengths near 405 nm, which are pertinent to common photoinitiators used in 3D printing. Accordingly, we chose to reduce lignin with $NaBH_4$ as a strategy to improve cure properties in lignin resins. In addition, these reductions have the added benefit of affording additional -OH groups in lignin, which we transform to append polymerizable acrylates. Similarly, acrylic anhydride was chosen as an alternate acylation method due to faster cure conversions in polyacrylates versus polymethacrylates [85].

Scheme 2. Reduction and acylation lignin modification.

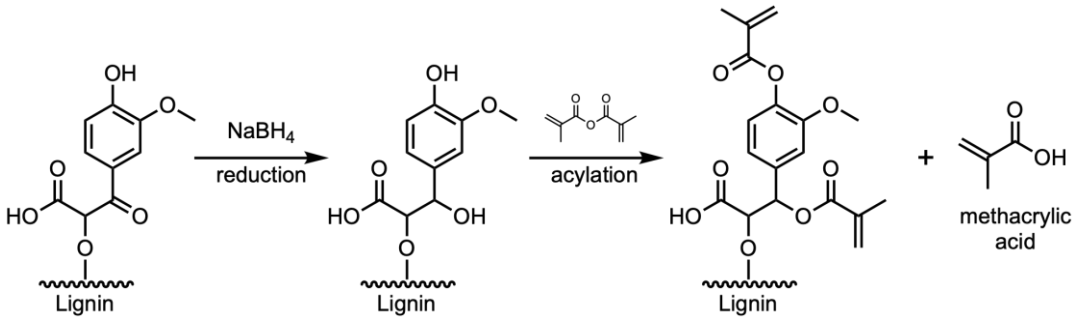

Characterization of Reduced and Acylated Lignin

Each type of modified lignin was characterized using FTIR, ^{31}P NMR, and UV-vis spectroscopies. Henceforth, these lignin samples will be label as Pine-M for methacrylic anhydride acylation, Pine-A for acrylic anhydride acylation, Pine-R for sodium borohydride reduction, and Pine-MR for reduction followed by methacrylic anhydride acylation. The FTIR spectra in Figure 9 show an increase in peak signal corresponding to C=O stretching, C–O–C stretching, and –CH_2 bending vibrations for acylated lignin samples (Pine-MR, Pine-A, and Pine-M) compared to the other samples. Likewise, these samples see a reduction in –OH functional groups. This confirms the success of the acylation reaction at the –OH sites.

We also used ^{31}P NMR spectroscopy to identify important changes to the structure of lignin. The results of these measurements are tabulated in Table 4. As expected, we detect a decrease in –OH groups among Pine-M, Pine-A, and Pine-MR, which indicates that the acylation reaction was successful. In addition, we detected a substantial increase in aliphatic –OH groups in Pine-R as compared to the unmodified lignin, which indicates $NaBH_4$ is capable of reducing aliphatic carbonyls in lignin to afford aliphatic –OH groups. These carbonyl groups have been implicated as chromophores that increase light absorption by lignin around 400 nm [84].

We also collected UV-vis absorption data in triplicate for lignin samples before and after each modification. These data, shown in Figure 10, indicate a significant decrease in absorption in the 380-450 nm range. At 405 nm, absorption decreased in Pine-M, Pine-A, and Pine-R by approximately 20-30%, while absorption decreased by greater than 60% in Pine-MR samples. We

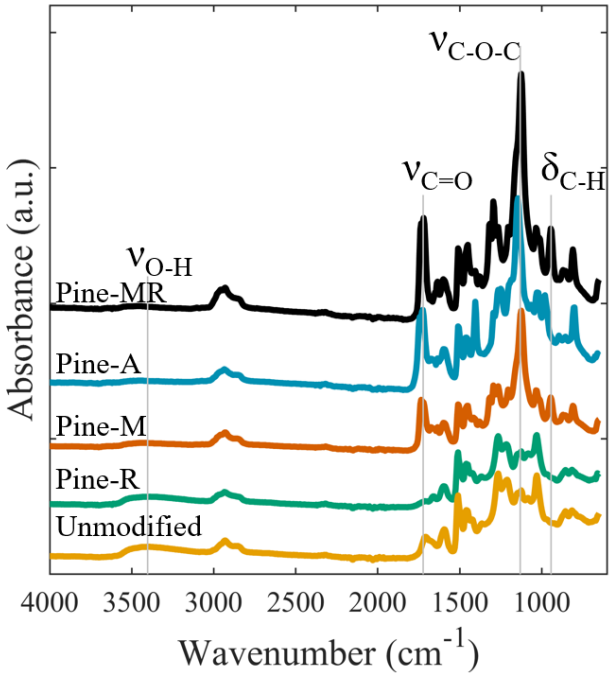

Figure 9. FTIR spectra for Pine lignin before and after each modification (top to bottom; Pine-MR, Pine-A, Pine-M, Pine-R, Unmodified).

Table 4. Hydroxyl content in mmol/g of lignin determined by ^{31}P NMR spectroscopy

Lignin	Aliphatic –OH	S –OH	G –OH	H –OH	–COOH
Unmodified	1.65	0.97	1.75	0.24	0.27
Pine-R	2.73	1.12	1.94	0.24	0.19
Pine-M	0.24	0.29	0.23	0.04	0.32
Pine-A	0.13	0.14	0.11	0.00	0.36
Pine-MR	0.25	0.11	0.06	0.01	0.19

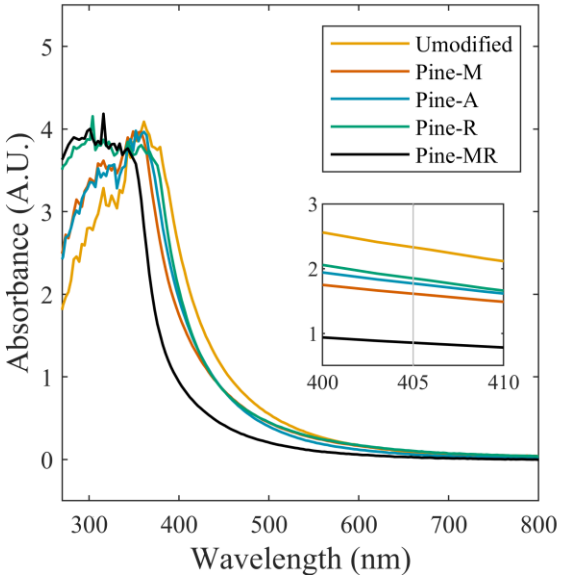

Figure 10. UV-vis absorption curves for modified Pine lignin showing UV absorption decrease. The inset shows difference in absorption at the 390-420 nm range.

chose chemical reduction as a strategy to decrease the number of chromophores in lignin. While the absorption curves show that this effect was achieved, acylation also evidently decreases absorption as well. While the exact reason for this change is unclear, we attribute it to an alteration in the electronic structure of lignin. In this way, acylation serves two purposes in lignin photopolymers: it is a means to append polymerizable groups to lignin and to also decrease the UV blocking effect imparted by unmodified lignin. Furthermore, it is perhaps unsurprising that the combination of acylation and chemical reduction improved the UV transparency more than any single modification technique, since chemical reduction affords additional reactive sites for acylation.

We performed size-exclusion chromatography on the lignin samples to observe the effect the reduction reaction had on molecular weight (MW). We note a negligible change in MW in reduced versus non-reduced samples. Pine-M has a number-average molecular weight M_n = 1279 g/mol and a weight-average molecular weight M_w = 3158 g/mol, while the reduced Pine-MR measures a M_n of 520 g/mol and a M_w of 2897 g/mol. This confirms that the reduction reaction

did not significantly alter the molecular weight of the lignin, which is useful information in characterizing material properties in the cured lignin resins.

Lignin Resins

We performed working curve calculations in triplicate using a window pane method outlined by Jacobs and modified as discussed above [27]. Figure 11 shows the resulting working curves and Table 5 shows the calculated fundamental resin parameters along with the dosage required to print 50 µm layer height with a 62 mW laser at 0.09 mm scan line spacing. We observe a slight improvement in cure properties of the Pine-A resin over Pine-M, which is reflected as a decrease in the calculated dosage per layer. The window pane technique evaluates cure reactivity as well as light penetration, so that could account for acrylate groups, which should be more reactive during free radical polymerization, exhibiting improved cure properties over methacrylate despite a negligible change in UV-vis measurements between Pine-M and Pine-A samples. A decrease in critical cure dosage and an increase in light penetration in the reduced lignin result in a significant change in the per-layer print dosage. Increasing values for light penetration correspond well to UV

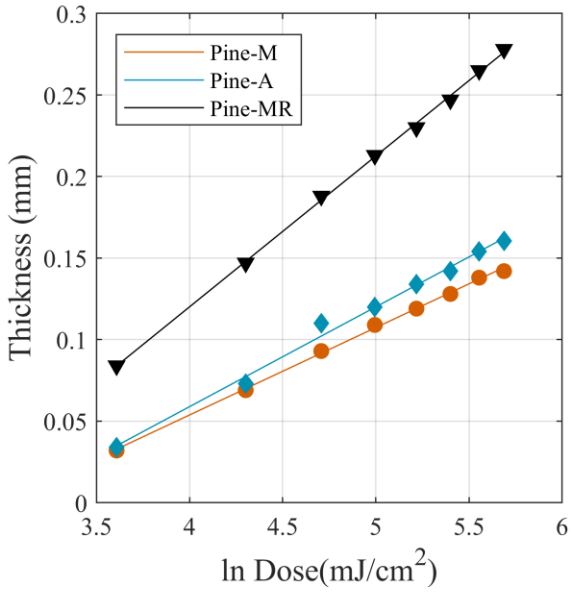

Figure 11. Working curves for lignin resins made with modified lignin. These are representative curves closest to the average of three tests.

Table 5. Cure parameters for tested resin formulations. The dosage is calculated per layer for a 50 µm layer height. Error on last digit shown in parenthesis.

Resin Formulation	D_p (mm)	E_c (mJ·cm^{-2})	Dosage (mJ·cm^{-2})
Base Resin	0.201(2)	23.7(1)	30(1)
Pine-M	0.054(1)	26.1(2)	66(1)
Pine-A	0.061(4)	24.9(2)	57(2)
Pine-MR	0.092(3)	18.6(2)	32(1)

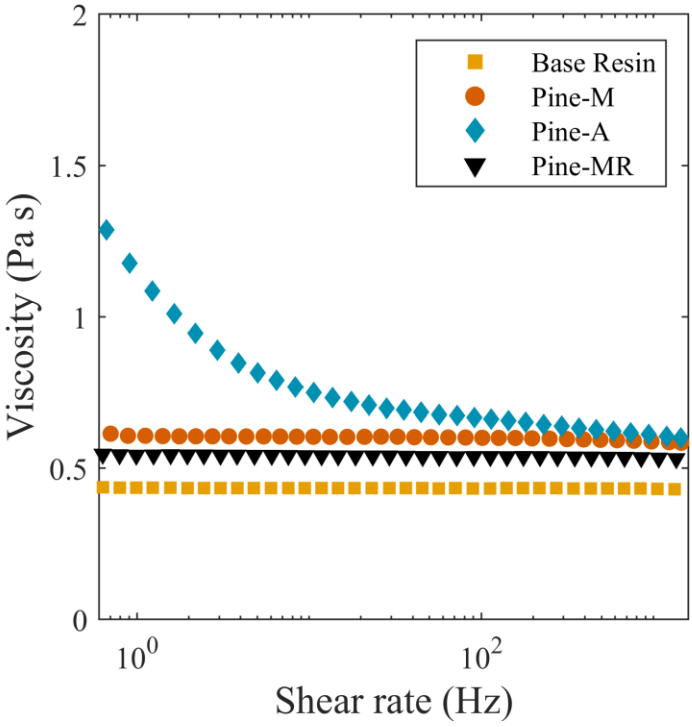

Figure 12. Viscosity versus shear rate for the base resin and lignin resins.

absorption data in all resins tested. Smaller critical cure dosages suggest improved reactivity in lignin resins. This could indicate that the changes in structure assist in lignin forming free radicals, potentially through the cleavage of aryl ether bonds like conventional photoinitiators [86, 87]. These changes move the required energy density in line with the target for printing based on commercial resins for the Pine-MR resin.

We also measured viscosity of all lignin resin samples, the results of which are shown in Figure 12. As expected, viscosity increases for all lignin resins compared to the base resin due to the introduction of the large lignin molecules. The Pine-A resins appears to shear thin at low shear rates before stabilizing at around 0.7 Pa s, which could be explained by poor incorporation between the modified lignin and the resin base components. All other resins exhibit Newtonian behavior in a range of approximately 0.4 to 0.6 Pa s, which we determine is an acceptable range for use in our printer. Pine-M and Pine-MR show stable viscosity measurements over a range of shear rates, indicating good dissolution in the resin base components.

Mechanical and Thermal Properties

We performed tensile testing of the casted resins to determine any mechanical difference imparted by the lignin modifications. The results of these tests are shown in Figure 13. We note an increase in modulus and tensile strength among all lignin samples compared to the base resin.

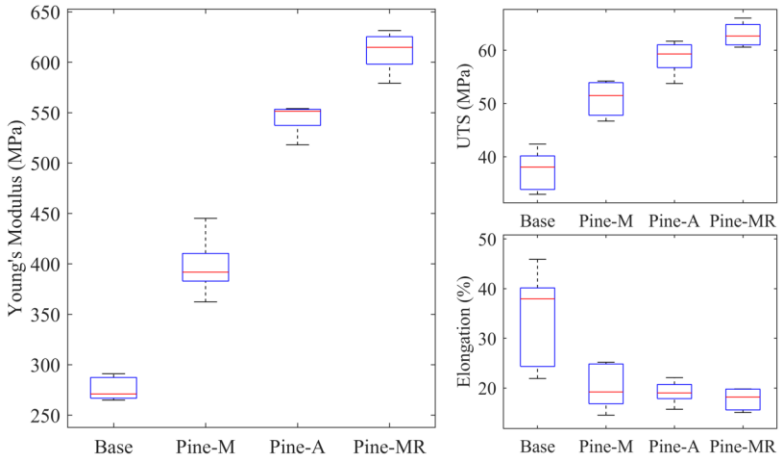

Figure 13. Young's modulus (A), ultimate tensile strength (B), and percent elongation (C) for casted base and lignin resins.

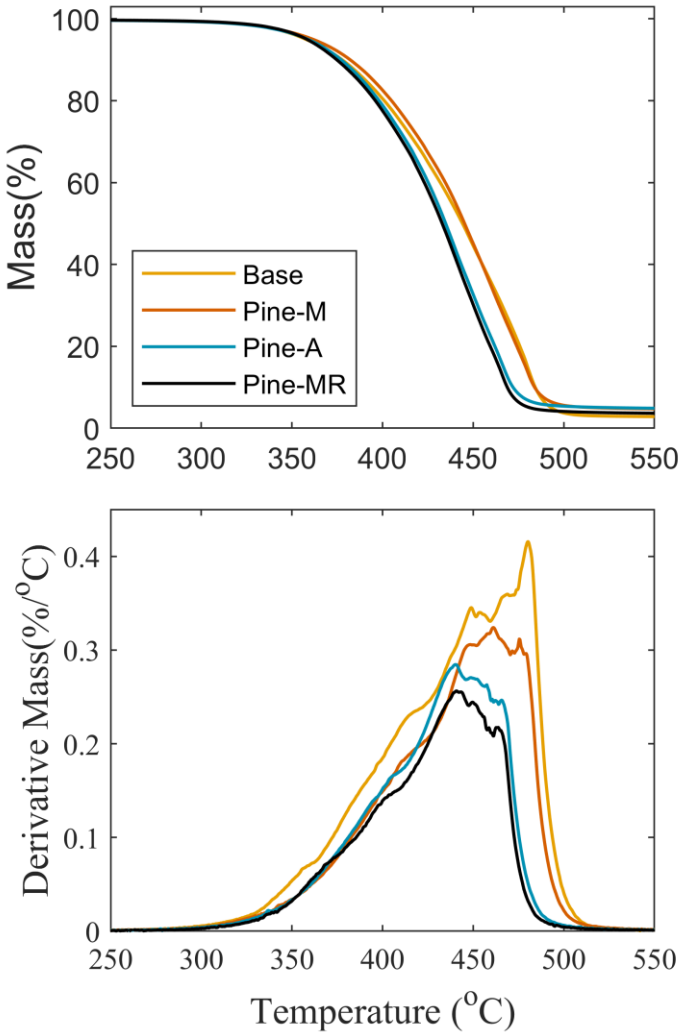

Figure 14. TGA (top) and DTGA (bottom) curves for base and lignin cured resins.

We attribute this to the increased crosslink density imparted by the multifunctional lignin-acrylates, which results in increased stiffness and strength and decreased ductility. Accordingly, Pine-MR is the stiffest and strongest casted resin, since it contains additional –OH groups from treatment with $NaBH_4$ and, as a result, the most acylated sites.

We also noted that Pine-A is stronger and stiffer than Pine-M. The UV-vis and Ec-Dp data above indicate that Pine-A is slightly more reactive than Pine-M, despite showing little improvement in UV transparency. Although the reason for this difference is unclear, we attribute the increases in stiffness and strength to improved crosslinking efficiency due to higher reactivity of acrylate when compared to methacrylate.

We performed thermogravimetric analysis (TGA) on the cured resins to evaluate changes in thermal behavior. The mass percent and derivative mass percent are shown in Figure 14. Although lignin has been shown previously to increase thermal stability in polymer composites, the lignin resins we report here decrease in the peak and onset differential decomposition temperatures compared to the base resin, particularly in Pine-A and Pine-MR resins [88]. We attribute this to the labile C–O bonds introduced by acylation of lignin that bind it to the polymer network [89]. DTGA curves shown in Figure 6b are unsurprisingly complex given the multicomponent polyurethane acrylate base resin. Random scission and depropagation reactions that have been observed in acrylic polymers and reformation of diisocynates and dialcohols in polyurethanes contribute to the complexity of the decomposition behaviors of these polymers [90-92].

3D Printing with Lignin Resin

We printed objects using Pine-MR lignin resin and a Formlabs Form 1+. We generated custom print settings to provide the dosage per layer calculated by the working curve calculations above. Macro images of these prints compared to the base resin are shown in Figure 15. The lignin prints exhibited rough faces and edges in contrast to the base resin print, which indicates worse x-y dimensional accuracy. Excess resin cured along the faces between the letters of the logo in the lignin resin print, and the top layer has a smoothing out of the edges that is not present in the model or in the base resin print. Likewise, artifacts can be seen on some of the lignin print faces, indicating inconsistent curing and shrinking in some layers.

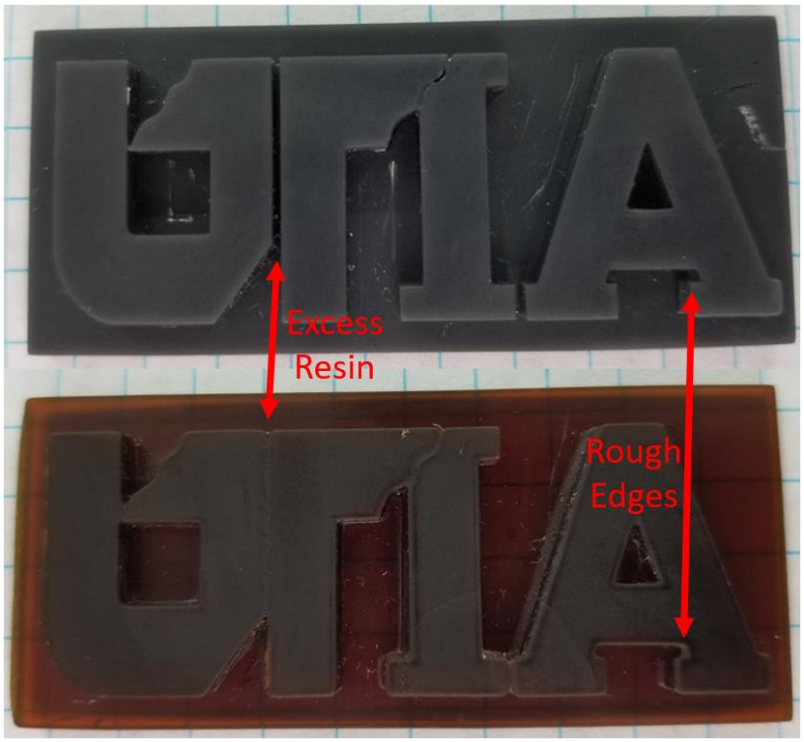

Figure 15. Base resin (top) and Pine-MR lignin resin (bottom) 3D printed logos shown with 1 cm separated gridlines.

Figure 16. Lignin resins pigmented (left to right) white, yellow, red, blue, black, none.

Visually, the lignin prints are dark brown-amber and are partially transparent. This is expected based on the UV-vis absorption data, which show opacity primarily in UV wavelengths. Due to this, it is possible to incorporate pigments into the resin formulation to achieve a limited range of colors, depending on the UV absorption of the pigments, as shown in Figure 16. This is important to the development of lignin polymers as the natural brown color is viewed unfavorably and considered a disadvantage to using lignin, especially in photopolymers where color additives can have significant effects on processing.

CONCLUSIONS

In this study, we evaluate the efficacy of different lignin modification techniques in reducing the UV absorption and improving cure properties in photo-active acrylate resins designed for SLA additive manufacturing. Fundamental resin parameters showed an increase in light penetration and a decrease in required cure dosage when comparing methacrylic acylation modification to acrylic and was improved further by a sodium borohydride reduction reaction prior to acylation. Lignin resins at 5 wt% loading showed an increase in Young's modulus and ultimate tensile strength in all case, with the highest increase for the reduced, methacrylated lignin. However, thermal stability was lowered compared to the base resin. Building on this study, future work will determine the lignin loading percent increased allowed by these modification techniques and evaluate the potential of pigmentation applied to lignin resins.

ACKNOWLEDGMENT

This project was supported by funds provided by the Southeastern Sun Grant Center and the US Department of Transportation, Research and Innovative Technology Administration DTOS59-07-G-00050. D.P.H. and S.C.C. acknowledge support from the USDA National Institute of Food and Agriculture, Hatch Project 1012359.

CHAPTER 4

CONCLUSIONS

CHAPTER CONCLUSIONS

Lignin has the potential to be a low-cost replacement for petroleum-based prepolymer components in 3D printing materials. The photoactive properties of lignin might be advantageous to photochemistry, but it can be a challenge to utilize them efficiently. Photopolymer resins used in additive manufacturing are generally highly engineered to operate correctly in the process used, so the properties of the lignin prepolymer material needs to be tunable to function within the tolerances of technology. Lignin extraction, modification, and characterization techniques were presented to provide context to lignin as a polymeric material. A discussion of additive manufacturing, particularly stereolithography, and photopolymer chemistry provide more background on the materials and processes used in this study. Although this work concentrates on stereolithography as the primary target application, lignin acrylates also have potential uses in photopolymer coatings and adhesives.

Chapter 2 focuses on the application of lignin to existing photo-active resins products using a commercial and open-source resin with a desktop SLA printer. A methacrylic anhydride modification technique was employed to acylate a hybrid poplar extracted lignin for incorporation in the polymer network. It was necessary to alter the control resin formulation to accommodate the UV blocking effect of lignin. Working curves were used to characterize resin parameters, which helped determine optimal print parameters for each formulation. The working curves showed a decrease in light penetration depth at the 405 nm wavelength with increasing lignin loading amounts. No significant change was observed in the critical cure dosage as lignin weight percent increased. Cured material was characterized using techniques discussed in Chapter 1. Thermal stability was reduced, which is attributed to the lability of the C–O bonds used to link lignin to the polymer network. Ductility was improved with additional lignin at the cost of a decrease in elastic modulus. Lignin resins were printed successfully at all loading amounts and exhibited high accuracy and good print quality. These results show that lignin can be substituted successfully for conventional prepolymer materials even in specialized photopolymer systems.

Chapter 3 focuses on an exploration of modification techniques to reduce the UV absorptivity at the cure wavelength range (395-415 nm). Pine lignin was extracted by an organosolv technique and modified using acylation and reduction. These materials were investigated using FTIR and ^{31}P NMR, confirming the reduction of highly oxidized moieties such

as ketones and aldehydes to OH groups and the appending of acrylic or methacrylic group to those sites. UV/vis spectroscopy showed a reduction in absorption at the target range for all modifications, with a significant decrease for the reduced, methacrylated lignin. Working curves for resins made with the modified lignin show overall dosage requirements in line with the absorption data. Critical cure dosage decreased more in the reduced lignin than the cure depth increased. This indicates that the improvements to cure properties result from the enhanced functionality of the reduced lignin over the lignin that was modified only by acylation. Mechanical characterization agrees with this; elastic modulus and tensile strength increase the most for the reduced and methacrylated lignin. TGA shows that peak decomposition temperatures are lower for acrylic anhydride modified lignin and reduced, methacrylic anhydride modified lignin. These results demonstrate the efficacy of using these chemical modifications to lignin to tune photoactive, mechanical, and thermal properties of lignin acrylate photopolymer materials.

IMPACT AND SIGNIFICANCE

The primary objective of this study is to evaluate and improve on the applicability of lignin to photopolymer resins for use in additive manufacturing. The recent growth of the additive manufacturing market over the last years in combination with increasing concerns of polymer waste and renewability have resulted in interest in developing novel materials that are competitive with conventional materials while also being more environmentally responsible and compatible with these new technologies. While lignin has been studied as a potential choice of filler material for polymers, the work presented here is novel for targeting SLA technology with lignin photopolymers. Acylation modification of extracted hybrid poplar lignin demonstrated that, even though lignin was detrimental to cure properties, it can be incorporated up to at least 15 percent by weight and still be in a reasonable cure dosage range. Lignin is usually dismissed outright from photocuring, so this is important for showing that it can be done.

Another significant aspect of this work is the evaluation of different chemical modifications to lignin, which include acylation and reduction, as a strategy to improve resin cure properties. This research shows that by disrupting the chromophoric groups in lignin, absorptivity in the UVA range can be decreased. It was also shown that these modifications had effects on mechanical and thermal properties of cured lignin resins. These results provide insight on the processing-structure-property relationship for the photoactivity and reactivity of lignin in these

polymer systems. This is important to the development of lignin-acrylate as it allows resin designs that tune properties to specific applications, which is enormously useful in these typically highly engineered photopolymers.

FUTURE WORK

This work will aid in the development of lignin acrylates and serve as a starting point for the design of new lignin-containing photo-active resins. Several topics still need further research to more efficiently use lignin in photopolymers and to determine in what specific applications it can be most useful. One such topic is the linking functional groups to lignin through C–C bonds instead of C–O bonds during modification to improve thermal stability of the resultant polymer. An investigation into modification techniques that can achieve this should be performed. Changes in chemical structure and functionality can be observed using spectroscopic techniques such as NMR, FTIR, and Raman spectroscopies. Cure kinetics of the modified material in a polymer resin can be evaluated using real-time infrared (RTIR) spectroscopy and dielectric analysis (DEA), and thermal properties of the cured material can be evaluated using differential scanning calorimetry (DSC) and TGA.

Acylation and reduction decreased UV absorption in lignin, but there are potential uses to lignin's photoactive properties in photopolymerization. A robust study of lignin's UVA and UVB absorptivity is necessary to determine its applicability as several components of conventional photopackages, namely as a UV blocker, photoinitiator, or pigment. UV/vis spectrophotometry needs to be performed along with Rayleigh scattering analysis to determine absorbance and scattering. This is critical to inform on what wavelength ranges lignin can be useful in and in what amounts for UV blockers and pigments. For photoinitiation, RTIR spectroscopy should also be used to evaluate cure conversion efficiency during resin polymerization. For this purpose, it is likely that carefully chosen components of depolymerized lignin would produce far better results than simply extracted lignin. Because isolating specific components can prove challenging, the initial stage of this investigation could use model compounds as stand-ins to first establish the feasibility of lignin-based photoinitiators.

With the progression of work done to enhance the cure properties of lignin-acrylates, it is necessary to reevaluate the optimal lignin loading amounts. Material properties will undoubtably vary significantly as the function of lignin in the polymer network changes from that of a

crosslinking agent to that of a prepolymer/oligomer. Rheological and mechanical studies, including measurement of viscosity, elastic and flexural moduli, and elongation, can shed light on lignin acrylate behavior with less influence from the other components of the resin formulation. These data will begin to fill out the material property spaces that lignin-acrylates can occupy and inform on applications, additive manufacturing or otherwise, that these materials can serve.

Building on that, sustainability and cost analyses should be done considering extraction and modification of lignin, production of lignin-acrylate resins, the application of the cured material, and the end-of-lifetime handling. Comparing this to conventional processing and materials will assist in deciding which purposes lignin is most suited to and how it can be incorporated in existing product streams. This work will guide the development of lignin as a desirable low-cost product on an industrial scale.

REFERENCES

[1] H. Chen, "Chemical Composition and Structure of Natural Lignocellulose," in *Biotechnology of Lignocellulose: Theory and Practice*, H. Chen, Ed. Dordrecht: Springer Netherlands, 2014, pp. 25-71.
[2] W. Boerjan, J. Ralph, and M. Baucher, "Lignin Biosynthesis," *Annual Review of Plant Biology*, vol. 54, no. 1, pp. 519-546, 2003.
[3] A. Sakakibara, "A structural model of softwood lignin," *Wood Science and Technology*, journal article vol. 14, no. 2, pp. 89-100, June 01 1980.
[4] F. R. D. van Parijs, K. Morreel, J. Ralph, W. Boerjan, and R. M. H. Merks, "Modeling Lignin Polymerization. I. Simulation Model of Dehydrogenation Polymers," *Plant Physiology*, vol. 153, no. 3, pp. 1332-1344, 2010.
[5] H. Tran and E. Vakkilainen, *THE KRAFT CHEMCIAL RECOVERY PROCESS*. 2016.
[6] F. S. Chakar and A. J. Ragauskas, "Review of current and future softwood kraft lignin process chemistry," *Industrial Crops and Products*, vol. 20, no. 2, pp. 131-141, 2004/09/01/ 2004.
[7] T. Joseph McDonough, *The chemistry of organosolv delignification*. 1993.
[8] Q. Schmetz *et al.*, "Comprehension of an organosolv process for lignin extraction on Festuca arundinacea and monitoring of the cellulose degradation," *Industrial Crops and Products*, vol. 94, pp. 308-317, 2016/12/30/ 2016.
[9] C. Nitsos *et al.*, "Isolation and Characterization of Organosolv and Alkaline Lignins from Hardwood and Softwood Biomass," *ACS Sustainable Chemistry & Engineering*, vol. 4, no. 10, pp. 5181-5193, 2016/10/03 2016.
[10] S. Laurichesse and L. Avérous, "Chemical modification of lignins: Towards biobased polymers," *Progress in Polymer Science*, vol. 39, no. 7, pp. 1266-1290, 2014/07/01/ 2014.
[11] M. P. Pandey and C. S. Kim, "Lignin Depolymerization and Conversion: A Review of Thermochemical Methods," *Chemical Engineering & Technology*, vol. 34, no. 1, pp. 29-41, 2011.
[12] Z. Sun, B. Fridrich, A. de Santi, S. Elangovan, and K. Barta, "Bright Side of Lignin Depolymerization: Toward New Platform Chemicals," *Chemical Reviews*, vol. 118, no. 2, pp. 614-678, 2018/01/24 2018.
[13] R. Ma, M. Guo, and X. Zhang, "Recent advances in oxidative valorization of lignin," *Catalysis Today*, vol. 302, pp. 50-60, 2018/03/15/ 2018.
[14] B. Xiao, X. F. Sun, and R. Sun, "The chemical modification of lignins with succinic anhydride in aqueous systems," *Polymer Degradation and Stability*, vol. 71, no. 2, pp. 223-231, 2001/01/01/ 2001.
[15] S. Yang, J.-L. Wen, T.-Q. Yuan, and R.-C. Sun, "Characterization and phenolation of biorefinery technical lignins for lignin–phenol–formaldehyde resin adhesive synthesis," *RSC Advances*, 10.1039/C4RA09595B vol. 4, no. 101, pp. 57996-58004, 2014.
[16] C. Ciobanu, M. Ungureanu, L. Ignat, D. Ungureanu, and V. I. Popa, "Properties of lignin–polyurethane films prepared by casting method," *Industrial Crops and Products*, vol. 20, no. 2, pp. 231-241, 2004/09/01/ 2004.
[17] M. Yakout and M. Elbestawi, *Additive Manufacturing of Composite Materials: An Overview*. 2017.
[18] M. L. Shofner, K. Lozano, F. J. Rodríguez-Macías, and E. V. Barrera, "Nanofiber-reinforced polymers prepared by fused deposition modeling," *Journal of Applied Polymer Science*, vol. 89, no. 11, pp. 3081-3090, 2003.
[19] P. D. Enrique, Y. Mahmoodkhani, E. Marzbanrad, E. Toyserkani, and N. Y. Zhou, "In situ formation of metal matrix composites using binder jet additive manufacturing (3D printing)," *Materials Letters*, vol. 232, pp. 179-182, 2018/12/01/ 2018.
[20] B. J. Holland and J. N. Hay, "The kinetics and mechanisms of the thermal degradation of poly(methyl methacrylate) studied by thermal analysis-Fourier transform infrared spectroscopy," *Polymer*, vol. 42, no. 11, pp. 4825-4835, 2001/05/01/ 2001.

[21] T. T. Wohlers and T. Caffrey, *Wohlers report 2015 : 3D printing and additive manufacturing state of the industry annual worldwide progress report*. Fort Collins, Colo.: Wohlers Associates, 2015.
[22] C. K. Chua, K. F. Leong, and Z. H. Liu, "Rapid tooling in manufacturing," *Handbook of Manufacturing Engineering and Technology*, pp. 1-22, 2013.
[23] J. Liu *et al.*, "Current and future trends in topology optimization for additive manufacturing," *Structural and Multidisciplinary Optimization*, vol. 57, no. 6, pp. 2457-2483, 2018/06/01 2018.
[24] B. Sagbas, *Additive Manufacturing of Biomedical Implants*. 2017.
[25] D. Bourell *et al.*, "Materials for additive manufacturing," *CIRP Annals*, vol. 66, no. 2, pp. 659-681, 2017/01/01/ 2017.
[26] S. Waheed *et al.*, "3D printed microfluidic devices: enablers and barriers," *Lab on a Chip*, 10.1039/C6LC00284F vol. 16, no. 11, pp. 1993-2013, 2016.
[27] P. F. Jacobs, D. T. Reid, Computer, and A. S. A. o. SME., *Rapid Prototyping & Manufacturing: Fundamentals of Stereolithography*. Society of Manufacturing Engineers, 1992.
[28] N. S. Allen, "Photoinitiators for UV and visible curing of coatings: Mechanisms and properties," *Journal of Photochemistry and Photobiology A: Chemistry*, vol. 100, no. 1, pp. 101-107, 1996/10/25/ 1996.
[29] J. T. Mehl, R. Murgasova, X. Dong, D. M. Hercules, and H. Nefzger, "Characterization of Polyether and Polyester Polyurethane Soft Blocks Using MALDI Mass Spectrometry," *Analytical Chemistry*, vol. 72, no. 11, pp. 2490-2498, 2000/06/01 2000.
[30] D. F. Swinehart, "The Beer-Lambert Law," *Journal of Chemical Education*, vol. 39, no. 7, p. 333, 1962/07/01 1962.
[31] H. G. M. Edwards, "IR and Raman Spectroscopies, The Study of Art Works☆," in *Encyclopedia of Spectroscopy and Spectrometry (Third Edition)*, J. C. Lindon, G. E. Tranter, and D. W. Koppenaal, Eds. Oxford: Academic Press, 2017, pp. 378-393.
[32] U. Holzgrabe, "Quantitative NMR, Methods and Applications," in *Encyclopedia of Spectroscopy and Spectrometry (Third Edition)*, J. C. Lindon, G. E. Tranter, and D. W. Koppenaal, Eds. Oxford: Academic Press, 2017, pp. 816-823.
[33] W. M. Groenewoud, "CHAPTER 2 - THERMOGRAVIMETRY," in *Characterisation of Polymers by Thermal Analysis*, W. M. Groenewoud, Ed. Amsterdam: Elsevier Science B.V., 2001, pp. 61-76.
[34] R. Hague, S. Mansour, N. Saleh, and R. Harris, "Materials analysis of stereolithography resins for use in Rapid Manufacturing," *Journal of Materials Science*, journal article vol. 39, no. 7, pp. 2457-2464, April 01 2004.
[35] F. N. Cogswell, "Chapter Two - Rheometry for Polymer Melts," in *Polymer Melt Rheology*, F. N. Cogswell, Ed.: Woodhead Publishing, 2003, pp. 15-38.
[36] M. Parit, P. Saha, V. A. Davis, and Z. Jiang, "Transparent and Homogenous Cellulose Nanocrystal/Lignin UV-Protection Films," *ACS Omega*, vol. 3, no. 9, pp. 10679-10691, 2018/09/30 2018.
[37] Y. Kim *et al.*, "All Biomass and UV Protective Composite Composed of Compatibilized Lignin and Poly (Lactic-acid)," (in eng), *Scientific Reports*, vol. 7, p. 43596, 2017.
[38] M. Ashby, "Hybrid Materials to Expand the Boundaries of Material-Property Space," (in English), *Journal of the American Ceramic Society*, Article vol. 94, pp. S3-S14, Jun 2011.
[39] S. S. Babu and R. Goodridge, "Additive manufacturing," *Materials Science and Technology*, vol. 31, no. 8, pp. 881-883, 2015/06/01 2015.
[40] F. P. W. Melchels, J. Feijen, and D. W. Grijpma, "A review on stereolithography and its applications in biomedical engineering," *Biomaterials*, vol. 31, no. 24, pp. 6121-6130, 2010/08/01/ 2010.
[41] I. Gibson, D. Rosen, and B. Stucker, *Additive Manufacturing Technologies: 3D Printing, Rapid Prototyping, and Direct Digital Manufacturing*. Springer New York, 2014.

[42] C. O. Tuck, E. Pérez, I. T. Horváth, R. A. Sheldon, and M. Poliakoff, "Valorization of Biomass: Deriving More Value from Waste," *Science,* vol. 337, no. 6095, pp. 695-699, 2012.
[43] P. Sannigrahi and A. Ragauskas, *Characterization of Fermentation Residues from the Production of Bio-Ethanol from Lignocellulosic Feedstocks*. 2011, pp. 514-519.
[44] A. J. Ragauskas *et al.*, "Lignin valorization: improving lignin processing in the biorefinery," (in eng), *Science,* vol. 344, no. 6185, p. 1246843, May 16 2014.
[45] B. M. Upton and A. M. Kasko, "Strategies for the Conversion of Lignin to High-Value Polymeric Materials: Review and Perspective," *Chemical Reviews,* vol. 116, no. 4, pp. 2275-2306, 2016/02/24 2016.
[46] F. H. M. Graichen *et al.*, "Yes, we can make money out of lignin and other bio-based resources," *Industrial Crops and Products,* vol. 106, pp. 74-85, 2017/11/01/ 2017.
[47] D. Nedelcu, N. M. Lohan, I. Volf, and R. Comaneci, "Thermal behaviour and stability of the Arboform® LV3 nature liquid wood," *Composites Part B: Engineering,* vol. 103, pp. 84-89, 2016/10/15/ 2016.
[48] N. A. Nguyen, C. C. Bowland, and A. K. Naskar, "A general method to improve 3D-printability and inter-layer adhesion in lignin-based composites," *Applied Materials Today,* vol. 12, pp. 138-152, 2018/09/01/ 2018.
[49] A. L. Holmberg, N. A. Nguyen, M. G. Karavolias, K. H. Reno, R. P. Wool, and T. H. Epps, "Softwood Lignin-Based Methacrylate Polymers with Tunable Thermal and Viscoelastic Properties," *Macromolecules,* vol. 49, no. 4, pp. 1286-1295, 2016/02/23 2016.
[50] A. L. Holmberg, K. H. Reno, N. A. Nguyen, R. P. Wool, and T. H. Epps, "Syringyl Methacrylate, a Hardwood Lignin-Based Monomer for High-Tg Polymeric Materials," *ACS Macro Letters,* vol. 5, no. 5, pp. 574-578, 2016/05/17 2016.
[51] D. J. van de Pas and K. M. Torr, "Biobased Epoxy Resins from Deconstructed Native Softwood Lignin," *Biomacromolecules,* vol. 18, no. 8, pp. 2640-2648, 2017/08/14 2017.
[52] K. Rajan *et al.*, "Sustainable Hydrogels Based on Lignin-Methacrylate Copolymers with Enhanced Water Retention and Tunable Material Properties," *Biomacromolecules,* vol. 19, no. 7, pp. 2665-2672, 2018/07/09 2018.
[53] H. Liu and H. Chung, "Visible-Light Induced Thiol–Ene Reaction on Natural Lignin," *ACS Sustainable Chemistry & Engineering,* vol. 5, no. 10, pp. 9160-9168, 2017/10/02 2017.
[54] J. J. Bozell, S. K. Black, M. Myers, D. Cahill, W. P. Miller, and S. Park, "Solvent fractionation of renewable woody feedstocks: Organosolv generation of biorefinery process streams for the production of biobased chemicals," *Biomass and Bioenergy,* vol. 35, no. 10, pp. 4197-4208, 2011/10/15/ 2011.
[55] M. Balakshin and E. Capanema, "On the Quantification of Lignin Hydroxyl Groups With 31P and 13C NMR Spectroscopy," *Journal of Wood Chemistry and Technology,* vol. 35, no. 3, pp. 220-237, 2015/05/04 2015.
[56] M. Schwanninger, J. C. Rodrigues, H. Pereira, and B. Hinterstoisser, "Effects of short-time vibratory ball milling on the shape of FT-IR spectra of wood and cellulose," *Vibrational Spectroscopy,* vol. 36, no. 1, pp. 23-40, 2004/10/18/ 2004.
[57] P. Lv, G. Almeida, and P. Perré, *TGA-FTIR Analysis of Torrefaction of Lignocellulosic Components (cellulose, xylan, lignin) in Isothermal Conditions over a Wide Range of Time Durations* (2015, no. 3). 2015.
[58] A. Udagawa, F. Sakurai, and T. Takahashi, "In situ study of photopolymerization by fourier transform infrared spectroscopy," *Journal of Applied Polymer Science,* vol. 42, no. 7, pp. 1861-1867, 1991.
[59] A. Castellan, S. Grelier, L. Kessab, A. Nourmamode, and Y. Hannachi, "Photophysics and photochemistry of a lignin model molecule containing α-carbonyl guaiacyl and 4-hydroxy-3-methoxybenzyl alcohol moieties," *Journal of the Chemical Society, Perkin Transactions 2,* 10.1039/P29960001131 no. 6, pp. 1131-1138, 1996.
[60] E. H. Immergut and H. F. Mark, "Principles of plasticization," ACS Publications, 1965.

[61] S. Kim *et al.*, "Computational Study of Bond Dissociation Enthalpies for a Large Range of Native and Modified Lignins," *The Journal of Physical Chemistry Letters*, vol. 2, no. 22, pp. 2846-2852, 2011/11/17 2011.
[62] L. Cao *et al.*, "Lignin valorization for the production of renewable chemicals: State-of-the-art review and future prospects," *Bioresource Technology*, vol. 269, pp. 465-475, 2018/12/01/ 2018.
[63] S. Kalami, M. Arefmanesh, E. Master, and M. Nejad, "Replacing 100% of phenol in phenolic adhesive formulations with lignin," *Journal of Applied Polymer Science*, vol. 134, no. 30, p. 45124, 2017.
[64] A. Mukhopadhyay, J. Hamel, R. Katahira, and H. Zhu, "Metal-Free Aqueous Flow Battery with Novel Ultrafiltered Lignin as Electrolyte," *ACS Sustainable Chemistry & Engineering*, vol. 6, no. 4, pp. 5394-5400, 2018/04/02 2018.
[65] A. A. Morandim-Giannetti, J. A. M. Agnelli, B. Z. Lanças, R. Magnabosco, S. A. Casarin, and S. H. P. Bettini, "Lignin as additive in polypropylene/coir composites: Thermal, mechanical and morphological properties," *Carbohydrate Polymers*, vol. 87, no. 4, pp. 2563-2568, 2012/03/01/ 2012.
[66] F. Avelino, D. R. de Oliveira, S. E. Mazzetto, and D. Lomonaco, "Poly(methyl methacrylate) films reinforced with coconut shell lignin fractions to enhance their UV-blocking, antioxidant and thermo-mechanical properties," (in eng), *Int J Biol Macromol*, vol. 125, pp. 171-180, Mar 15 2019.
[67] W. Huang, M. Wu, W. Liu, Z. Hua, Z. Wang, and L. Zhou, "Value-adding of organosolv lignin: Designing mechanically robust UV-resistant polymeric glass via ARGET ATRP," *Applied Surface Science*, vol. 475, pp. 302-311, 2019/05/01/ 2019.
[68] S. C. Lee, T. M. T. Tran, J. W. Choi, and K. Won, "Lignin for white natural sunscreens," *International Journal of Biological Macromolecules*, vol. 122, pp. 549-554, 2019/02/01/ 2019.
[69] Y. Qian, X. Qiu, and S. Zhu, "Lignin: a nature-inspired sun blocker for broad-spectrum sunscreens," *Green Chemistry*, 10.1039/C4GC01333F vol. 17, no. 1, pp. 320-324, 2015.
[70] Y. Qian, X. Qiu, and S. Zhu, "Sunscreen Performance of Lignin from Different Technical Resources and Their General Synergistic Effect with Synthetic Sunscreens," *ACS Sustainable Chemistry & Engineering*, vol. 4, no. 7, pp. 4029-4035, 2016/07/05 2016.
[71] N.-E. E. Mansouri and J. Salvadó, "Structural characterization of technical lignins for the production of adhesives: Application to lignosulfonate, kraft, soda-anthraquinone, organosolv and ethanol process lignins," *Industrial Crops and Products*, vol. 24, no. 1, pp. 8-16, 2006/07/01/ 2006.
[72] J. Domínguez-Robles, T. Tamminen, T. Liitiä, M. S. Peresin, A. Rodríguez, and A.-S. Jääskeläinen, "Aqueous acetone fractionation of kraft, organosolv and soda lignins," *International Journal of Biological Macromolecules*, vol. 106, pp. 979-987, 2018/01/01/ 2018.
[73] C. Nitsos, U. Rova, and P. Christakopoulos, "Organosolv fractionation of softwood biomass for biofuel and biorefinery applications," *Energies*, vol. 11, no. 1, p. 50, 2017.
[74] S. Chatterjee and T. Saito, "Solvent Fractionation of Lignin," in *Polymer Precursor-Derived Carbon*, vol. 1173(ACS Symposium Series, no. 1173): American Chemical Society, 2014, pp. 153-168.
[75] X. Jiang, J. Liu, X. Du, Z. Hu, H.-m. Chang, and H. Jameel, "Phenolation to Improve Lignin Reactivity toward Thermosets Application," *ACS Sustainable Chemistry & Engineering*, vol. 6, no. 4, pp. 5504-5512, 2018/04/02 2018.
[76] D. Kun and B. Pukánszky, "Polymer/lignin blends: Interactions, properties, applications," *European Polymer Journal*, vol. 93, pp. 618-641, 2017/08/01/ 2017.
[77] J. V. Crivello and E. Reichmanis, "Photopolymer Materials and Processes for Advanced Technologies," *Chemistry of Materials*, vol. 26, no. 1, pp. 533-548, 2014/01/14 2014.
[78] A. Pansky *et al.*, "Non-toxic flexible photopolymers for medical stereolithography technology," *Rapid Prototyping Journal*, vol. 13, no. 1, pp. 38-47, 2007/01/23 2007.

[79] M. Lebedevaite, J. Ostrauskaite, E. Skliutas, and M. Malinauskas, "Photoinitiator Free Resins Composed of Plant-Derived Monomers for the Optical μ-3D Printing of Thermosets," *Polymers,* vol. 11, no. 1, p. 116, 2019.
[80] R. Ding, Y. Du, R. B. Goncalves, L. F. Francis, and T. M. Reineke, "Sustainable near UV-curable acrylates based on natural phenolics for stereolithography 3D printing," *Polymer Chemistry,* 10.1039/C8PY01652F vol. 10, no. 9, pp. 1067-1077, 2019.
[81] J. T. Sutton, K. Rajan, D. P. Harper, and S. C. Chmely, "Lignin-Containing Photoactive Resins for 3D Printing by Stereolithography," *ACS Applied Materials & Interfaces,* vol. 10, no. 42, pp. 36456-36463, 2018/10/24 2018.
[82] M. H. Langholtz *et al.*, "2016 Billion-ton report: advancing domestic resources for a thriving bioeconomy, volume 1: economic availability of feedstocks," Oak Ridge National Lab.(ORNL), Oak Ridge, TN (United States)2016.
[83] V. García-Negrón *et al.*, "Processing–Structure–Property Relationships for Lignin-Based Carbonaceous Materials Used in Energy-Storage Applications," *Energy Technology,* vol. 5, no. 8, pp. 1311-1321, 2017/08/01 2017.
[84] S. I. Falkehag, J. Marton, and E. Adler, "Chromophores in Kraft Lignin," in *Lignin Structure and Reactions*, vol. 59(Advances in Chemistry, no. 59): AMERICAN CHEMICAL SOCIETY, 1966, pp. 75-89.
[85] J. F. G. A. Jansen, A. A. Dias, M. Dorschu, and B. Coussens, "Fast Monomers: Factors Affecting the Inherent Reactivity of Acrylate Monomers in Photoinitiated Acrylate Polymerization," *Macromolecules,* vol. 36, no. 11, pp. 3861-3873, 2003/06/01 2003.
[86] C. Amen-Chen, H. Pakdel, and C. Roy, "Production of monomeric phenols by thermochemical conversion of biomass: a review," *Bioresource Technology,* vol. 79, no. 3, pp. 277-299, 2001/09/01/ 2001.
[87] W. A. Green, *Industrial photoinitiators: a technical guide*. CRC Press, 2010.
[88] S. Sen, S. Patil, and D. S. Argyropoulos, "Thermal properties of lignin in copolymers, blends, and composites: a review," *Green Chemistry,* 10.1039/C5GC01066G vol. 17, no. 11, pp. 4862-4887, 2015.
[89] P. F. Britt, A. C. Buchanan, M. J. Cooney, and D. R. Martineau, "Flash Vacuum Pyrolysis of Methoxy-Substituted Lignin Model Compounds," *The Journal of Organic Chemistry,* vol. 65, no. 5, pp. 1376-1389, 2000/03/01 2000.
[90] A. H. Ali and K. S. V. Srinivasan, "Studies on the Thermal Degradation of Acrylic Polymers by Simultaneous Autostep TG/DTA," *Journal of Macromolecular Science, Part A,* vol. 34, no. 2, pp. 235-246, 1997/02/01 1997.
[91] A. Ballistreri, S. Foti, P. Maravigna, G. Montaudo, and E. Scamporrino, "Mechanism of thermal degradation of polyurethanes investigated by direct pyrolysis in the mass spectrometer," *Journal of Polymer Science: Polymer Chemistry Edition,* vol. 18, no. 6, pp. 1923-1931, 1980.
[92] J. Chambers, J. Jiricny, and C. B. Reese, "The thermal decomposition of polyurethanes and polyisocyanurates," *Fire and Materials,* vol. 5, no. 4, pp. 133-141, 1981.

VITA

Jordan Sutton was born in Memphis, Tennessee on April 4, 1995. He obtained his Bachelor of Science in Materials Science and Engineering from the University of Tennessee-Knoxville in May 2017. Prior to earning his bachelor's degree, he interned at Osmose chemical plant in Millington, Tennessee documenting work and safety procedures. He also performed research under Dr. Gajanan Bhat at UT's Nonwovens Research Laboratory. He worked on preparing and characterizing nonwoven and fiber materials from recycled polymers. During his last undergraduate years, he manufactured and tested fiber composite materials with the Institute for Advanced Composite Manufacturing Innovation group at UT under Dr. Uday Vaidya. In the fall of 2017, he joined Dr. Stephen Chmely and Dr. David Harper at UT's Center for Renewable Carbon to obtain his Master of Science degree in Materials Science and Engineering. He plans to finish his master's degree in the summer of 2019 and then find industry work in polymer manufacturing.